NASA/CR—2003-212298

Aircraft Engine Sensor/Actuator/Component Fault Diagnosis Using a Bank of Kalman Filters

Takahisa Kobayashi
QSS Group, Inc., Cleveland, Ohio

March 2003

The NASA STI Program Office . . . in Profile

Since its founding, NASA has been dedicated to the advancement of aeronautics and space science. The NASA Scientific and Technical Information (STI) Program Office plays a key part in helping NASA maintain this important role.

The NASA STI Program Office is operated by Langley Research Center, the Lead Center for NASA's scientific and technical information. The NASA STI Program Office provides access to the NASA STI Database, the largest collection of aeronautical and space science STI in the world. The Program Office is also NASA's institutional mechanism for disseminating the results of its research and development activities. These results are published by NASA in the NASA STI Report Series, which includes the following report types:

- TECHNICAL PUBLICATION. Reports of completed research or a major significant phase of research that present the results of NASA programs and include extensive data or theoretical analysis. Includes compilations of significant scientific and technical data and information deemed to be of continuing reference value. NASA's counterpart of peer-reviewed formal professional papers but has less stringent limitations on manuscript length and extent of graphic presentations.

- TECHNICAL MEMORANDUM. Scientific and technical findings that are preliminary or of specialized interest, e.g., quick release reports, working papers, and bibliographies that contain minimal annotation. Does not contain extensive analysis.

- CONTRACTOR REPORT. Scientific and technical findings by NASA-sponsored contractors and grantees.

- CONFERENCE PUBLICATION. Collected papers from scientific and technical conferences, symposia, seminars, or other meetings sponsored or cosponsored by NASA.

- SPECIAL PUBLICATION. Scientific, technical, or historical information from NASA programs, projects, and missions, often concerned with subjects having substantial public interest.

- TECHNICAL TRANSLATION. English-language translations of foreign scientific and technical material pertinent to NASA's mission.

Specialized services that complement the STI Program Office's diverse offerings include creating custom thesauri, building customized databases, organizing and publishing research results . . . even providing videos.

For more information about the NASA STI Program Office, see the following:

- Access the NASA STI Program Home Page at ***http://www.sti.nasa.gov***

- E-mail your question via the Internet to help@sti.nasa.gov

- Fax your question to the NASA Access Help Desk at 301–621–0134

- Telephone the NASA Access Help Desk at 301–621–0390

- Write to:
  NASA Access Help Desk
  NASA Center for AeroSpace Information
  7121 Standard Drive
  Hanover, MD 21076

NASA/CR—2003-212298

Aircraft Engine Sensor/Actuator/Component Fault Diagnosis Using a Bank of Kalman Filters

Takahisa Kobayashi
QSS Group, Inc., Cleveland, Ohio

Prepared under Contract NAS3–00145

National Aeronautics and
Space Administration

Glenn Research Center

March 2003

Acknowledgments

This research was funded by the NASA Aviation Safety Program as a task under the Propulsion System Health Management Element. The NASA technical representative was Donald L. Simon of U.S. Army Research Laboratory at Glenn Research Center, Cleveland, Ohio.

Available from

NASA Center for Aerospace Information
7121 Standard Drive
Hanover, MD 21076

National Technical Information Service
5285 Port Royal Road
Springfield, VA 22100

Available electronically at http://gltrs.grc.nasa.gov

Aircraft Engine Sensor/Actuator/Component Fault Diagnosis Using a Bank of Kalman Filters

Takahisa Kobayashi
QSS Group, Inc
Cleveland, Ohio 44135

Executive Summary

In this report, a fault detection and isolation (FDI) system which utilizes a bank of Kalman filters is developed for aircraft engine sensor and actuator FDI in conjunction with the detection of component faults. This FDI approach uses multiple Kalman filters, each of which is designed based on a specific hypothesis for detecting a specific sensor or actuator fault. In the event that a fault does occur, all filters except the one using the correct hypothesis will produce large estimation errors, from which a specific fault is isolated. In the meantime, a set of parameters that indicate engine component performance is estimated for the detection of abrupt degradation. The performance of the FDI system is evaluated against a nonlinear engine simulation for various engine faults at cruise operating conditions. In order to mimic the real engine environment, the nonlinear simulation is executed not only at the nominal, or healthy, condition but also at aged conditions. When the FDI system designed at the healthy condition is applied to an aged engine, the effectiveness of the FDI system is impacted by the mismatch in the engine health condition. Depending on its severity, this mismatch can cause the FDI system to generate incorrect diagnostic results, such as false alarms and missed detections. To partially recover the nominal performance, two approaches, which incorporate information regarding the engine's aging condition in the FDI system, will be discussed and evaluated. The results indicate that the proposed FDI system is promising for reliable diagnostics of aircraft engines.

Nomenclature

A16 : Variable bypass duct area
A8 : Nozzle area
BST : Booster
CLM : Component Level Model
FAN : Fan
FDI : Fault detection and isolation
FOD : Foreign object damage
HPC : High-pressure compressor
HPT : High-pressure turbine
LPT : Low-pressure turbine
P27 : HPC inlet pressure
PS15 : Bypass duct static pressure
PS3 : Combustor inlet static pressure
PS56 : LPT exit static pressure
T27D : Booster inlet temperature
T56 : LPT exit temperature
TMPC : Burner exit heat soak (metal temp.)
WF36 : Fuel flow
XN2 : Low-pressure spool speed, measured
XN25 : High-pressure spool speed, measured
XNH : High-pressure spool speed, state variable
XNL : Low-pressure spool speed, state variable

1.0 Introduction

Fault detection and isolation (FDI) logic is critical to the safe and reliable operation of aircraft gas turbine engines. It is desirable to detect and identify any fault as soon as possible so that the scenario of a minor fault escalating into a more serious failure can be avoided. However, achieving the FDI task with high reliability is a challenging problem. Faults may occur in various degrees of severity at various locations; therefore numerous fault scenarios are possible. Moreover, the engine's complex structure and harsh operating environment make interpretation of the available information difficult. For instance, the sensor measurements from which the FDI decision is made can often be unreliable due to bias or intense noise. To deal with such problems, the introduction of analytical redundancy has become common and is considered more cost-effective than hardware redundancy. With the increase of digital computational power, more sophisticated approaches such as the utilization of an on-board engine model have become possible.

In this paper, a model-based approach utilizing a bank of Kalman filters is investigated for aircraft engine sensor and actuator FDI in conjunction with the detection of component faults. This approach uses multiple Kalman filters each of which is designed for detecting a specific sensor or actuator fault. In the event that a fault does occur, all filters except the one using the correct hypothesis will produce large estimation errors. By monitoring the residual of each filter, the specific fault that has occurred can be detected and isolated. In the meantime, a set of parameters which indicate engine component performance is estimated for the detection of abrupt degradation. This FDI logic is currently stand-alone and is not integrated with a control system. Therefore, fault accommodation is not discussed although failed sensor measurements and true actuator positions are estimated to ensure that further sensor/actuator accommodation steps are possible. The proposed FDI logic is applied to a nonlinear engine simulation and evaluated for various engine faults at cruise operating conditions. In order to mimic the real engine environment, the nonlinear simulation is executed not only at the nominal, or healthy, condition but also at the aged conditions. Although the effectiveness of the FDI system is impacted by aging engine effects, two approaches to recover the performance will be discussed and evaluated.

2.0 Background of Fault Detection and Isolation

When a fault occurs, the first step is to detect it as soon as possible. The approach commonly used for model-based fault detection is composed of two steps: 1) generate residual signals from the sensor measurements and their estimated values, and then 2) compare the residuals with thresholds to make fault detection decisions.[1] Sensor noise and modeling uncertainty are key factors that affect detection performance. A fault signature contained in the measurements is often corrupted by sensor noise, and un-modeled engine dynamics may generate a fault-like signature. These factors lead to missed detections and false alarms. To reduce the effects of noise, the sensor measurements can be averaged over a given length of time (i.e., window averaging). Although this approach may remove spike-like fault signatures, it can retain fault information which spans a period of time. To deal with modeling uncertainty, robust detection approaches have been investigated by some researchers.[2,3,4] In the robust design approach, modeling uncertainty is accounted for in the residual generation process. Therefore, a fault detection system can be sensitive to faults while being robust to modeling uncertainty.

In the study done by Khargonekar et al.[4], a fault detection approach was investigated in the presence of modeling uncertainty with the following two assumptions: 1) a weighting transfer function that bounds the modeling uncertainty magnitude is known, and 2) complete knowledge of all possible failure signals is available. In this study, the difference between the weighted partial $L2$ norm of input signal and that of

the output signal of a normalized system is computed. The weighted partial $L2$ norm indicates the energy of the signal. Therefore, if the output energy exceeds the input energy by some amount, it indicates that a fault has occurred in a system.

In Patton et al.[2], an observer-based robust sensor fault detection approach was applied to a jet engine simulation. In order to decouple the effects that uncertainties and faults have on the system being monitored, all uncertainties are treated as disturbances acting on the system. An important assumption made in this approach is that the disturbance (uncertainty) distribution matrix is known. Although a generalized approach to determine this matrix is not available, a technique to estimate such a matrix is discussed in this and other references.[5,6] The robust sensor fault detection approach was demonstrated under the presence of modeling uncertainty and parameter variations due to changes in the operating point.

Once a fault is successfully detected, the next step is to isolate the particular fault from other potential faults. A single fault isolation technique for aircraft engine performance diagnostics was investigated by Volponi et al.[7] Assuming that a fault has already been detected, this approach processed Kalman filter equations iteratively for each of the root causes under consideration and subsequently ranked fault candidates in order of likelihood based on the estimation error norms. The application of a bank of estimators for fault detection and isolation was conducted by Merrill et al.[8], Duyar et al.[9], and Menke et al.[10] This approach uses multiple estimators, each of which is designed for detecting a specific fault. Since each estimator is designed based on a specific hypothesis (such as the failure of a single sensor or actuator), all estimators except the one using the correct hypothesis will produce large estimation errors when a fault occurs. By monitoring the residual of each estimator, the specific fault that has occurred can be detected and isolated.

In the study done by Merrill et al.[8], a bank of Kalman filters was applied for aircraft engine sensor FDI. This study successfully demonstrated improved control loop tolerance to sensor failures (bias and drift), which were considered the most likely engine failures to happen under the harsh operating environment. Those sensors used in the control loop were monitored and accommodated in the event of failure. In this study, actuation failure was not considered.

In Duyar et al.[9], a fault detection and diagnosis (FDD) system was developed and applied to the Space Shuttle main engine simulation for actuator, sensor, and component faults. A bank of three hypothesis testing modules, each of which was designed for a specific fault category (actuator, sensor, or component category), was utilized for fault isolation. Each module identified specific fault parameters followed by the construction of output estimates. The validity of the FDD system was successfully demonstrated for actuator and sensor fault cases in the simulation environment. However, it was noted that further research is needed to achieve the component fault diagnosis.

In the study done by Menke et al.[10], a bank of Kalman filters was applied to detect and isolate hard failures in sensors and actuators of the F-16 aircraft. In this study, the faults were assumed to be known; the hard failure was modeled by zeroing out a row or a column of the state space matrices corresponding to the failed sensor or actuator. Kalman filters were designed for the possible sensor and actuator faults. With the assumption that the sensors and actuators can fail one at a time, the outputs of Kalman filters were used for computing the conditional probability from which a failed or non-failed decision was made. It was noted that this approach requires a stimulus, such as control surface perturbations, for disturbing the system in order to generate adequate growth in the residual signals.

The detection and isolation of soft actuator failures is a challenging problem. In the problem setup for model-based estimators such as Kalman filter, it is assumed that actuators are properly configured to their commanded positions so that plant responses to actuator perturbations are canceled out in the estimation

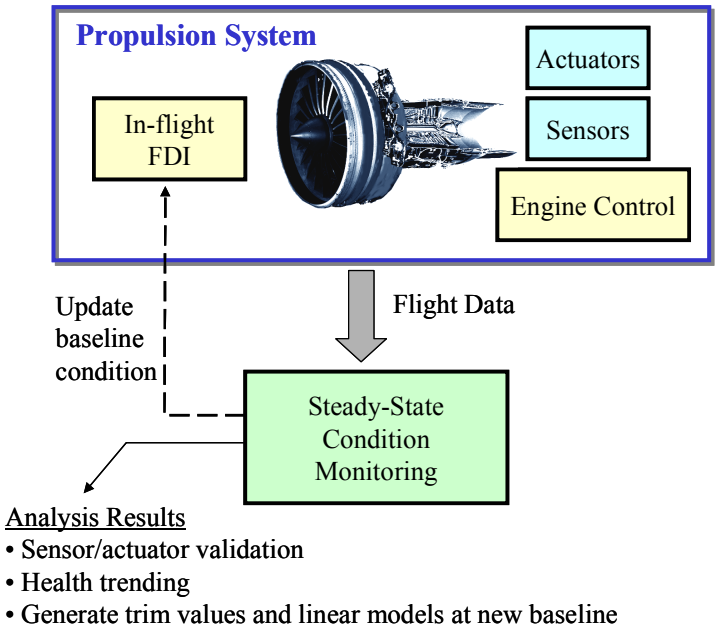

Figure 1. Structure of the Propulsion Health Management System

loop. Obviously, if there is a large difference between true and commanded actuator positions, this discrepancy will result in estimation error. Unlike the bank-of-filters approach for sensor FDI where one sensor is excluded from the sensor suite for each detection filter design, an actuator position or command signal cannot be excluded for its failure detection. Therefore, a different approach is needed for actuator FDI.

In Hajiyev et al.[11], a Kalman filter was applied for aircraft sensor and actuator fault diagnosis. This approach was based on an assumption that the statistics of a faulty sensor would change much more than those of the other sensors. A sensor fault that shifted the mean of the innovation sequence could be detected and isolated. However, actuator fault diagnosis was not successful.

3.0 Approach to Propulsion Health Management

The FDI logic discussed in this paper is a part of the Propulsion Health Management System (PHMS) investigated at NASA Glenn Research Center. The PHMS is composed of two parts: 1) steady-state condition monitoring, and 2) real-time in-flight FDI logic. The PHMS architecture is shown in Figure 1.

The steady-state condition monitoring is conducted using steady-state flight data. The monitoring system can be on-board or ground-based. The objective of condition monitoring is achieved by accurately estimating a set of unmeasurable parameters that indicate the engine health condition. These parameters are referred to as "health parameters." By accurately tracking the health parameter deterioration from the nominal, or healthy, baseline condition, proper maintenance can be performed as needed. However, accurately estimating the health parameters is a challenging problem because of several issues. First, the

sensor and actuator measurements, from which the health parameters are estimated, may be distorted by bias. Estimation techniques often attribute a measurement bias to a component health degradation which may lead to an incorrect conclusion; therefore the pre-validation of measurements is critical. Secondly, the location and the number of sensors limit the number of health parameters that can be estimated accurately. The number of health parameters often exceeds the number of available sensors, and the observability of some parameters may be limited due to sensor location. To partially deal with the underdetermined condition, flight data at multiple operating points[12] or the past trend of component condition[13] may be used. Finally, the combination of the above issues and highly nonlinear engine dynamics may result in multiple health degradation scenarios producing similar measurement shifts. In such a case, ranking the probable solutions[14] and further investigation may be necessary to avoid making a decision based on an incorrect estimation. Achieving accurate estimation in the presence of the above issues is a time consuming process. This process time may not be so critical for trend monitoring since engine degradation due to aging progresses gradually in general. However, it would be beneficial if the estimation process could be completed for each flight leg.

The steady-state condition monitoring approach developed in previous in-house research[15] at NASA Glenn Research Center utilized a nonlinear engine model, neural networks, and genetic algorithms for health parameter estimation and validation. The nonlinear engine model was used as analytical redundancy of an entire engine and tuned based on the health condition estimated by neural networks and genetic algorithms. This approach fulfills the first part of the PHMS. The focus of the current study is the second part of the PHMS: the development of real-time in-flight FDI logic. An FDI system will be developed using a linear estimation approach and applied to a nonlinear engine simulation for performance evaluation.

Engine Model

The engine model being used for in-house research is the nonlinear simulation of an advanced military twin-spool turbofan engine.[16] This simulation is constructed as a Component Level Model (CLM), which assembles the major components of an aircraft engine. Engine performance deterioration is modeled by adjustments to efficiency and/or flow coefficient scalars of the following five components: Fan (FAN), Booster (BST), High-Pressure Compressor (HPC), High-Pressure Turbine (HPT), and Low-Pressure Turbine (LPT). These scalars representing the component performance deterioration are the health parameters. The engine state variables, health parameters, actuation variables, and sensor measurements used in the current research are shown in Table 1. The actuator dynamics are much faster than the engine dynamics, and therefore the actuator state variables are ignored.

Engine Component Baseline Degradation Versus Component Fault

It is well known that the physical engine components deteriorate gradually due to wear and tear on blades and the casing as an engine operates over time.[17,18,19,20,21] In this paper, such gradual component deterioration due to aging is referred to as “baseline degradation” and represented by deviations in all 10 health parameters from the healthy baseline condition. As discussed, the baseline degradation can be tracked by steady-state condition monitoring systems. Besides this gradual process of deterioration, the health parameters may also degrade abruptly during a mission flight due to incidents such as foreign object damage (FOD). Such abrupt degradation is defined as “component fault” in this paper. The objective of the FDI system to be developed is to detect component faults in addition to sensor and actuator FDI.

Table 1. State Variables, Health Parameters, Actuators, and Sensors of the Engine Model

State Variables	Health Parameters	Actuators	Sensors
XNL	FAN efficiency	WF36	XN2
XNH	FAN flow capacity	A8	XN25
TMPC	BST efficiency	A16	T27D
	BST flow capacity		T56
	HPC efficiency		PS15
	HPC flow capacity		P27
	HPT efficiency		PS3
	HPT flow capacity		PS56
	LPT efficiency		
	LPT flow capacity		

As shown in Figure 1, the FDI system is integrated with the steady-state condition monitoring system developed in the previous research in order to improve its robustness to variations in the baseline condition. After the completion of the steady-state condition monitoring process in which the nonlinear engine model is tuned based on estimated baseline degradation, the trim values at the new baseline condition and a linear state-space model are extracted from the nonlinear engine model. The extracted information is then used to design or update the FDI system so that the baseline condition of the FDI system will match with that of an operational (aging) engine. In the later section, the approaches for integrating the FDI system with the steady-state condition monitoring system will be discussed in detail.

4.0 Development of Fault Detection and Isolation Logic

A depiction of the FDI logic integrated with the propulsion system is shown in Figure 2. The FDI logic uses two sets of input signals; sensor measurements and control commands. Sensor measurements are corrupted by noise and may be faulty due to sensor failure. Actuators may also experience mechanical and/or electrical failures. As shown in Figure 2, the FDI logic uses control commands (u_{cmd}). Alternatively, the true actuator positions (u_{true}) may be directly measured, and the sensed values may be used by the FDI logic. However, using sensed actuator positions would add complexity to the FDI problem, since an actuator fault can happen not only to an actuator itself but also to an actuator position feedback sensor. Therefore, an actuator failure is simply defined as an inconsistency between true actuator position and control command. The sensor and actuator failures dealt with in this paper are so-called "soft" failures. Soft failures are defined as inconsistencies between true and measured sensor values (or true and commanded actuator values) that are relatively small in magnitude and thus difficult to detect by a simple range-checking approach, whereas "hard" failures are larger in magnitude and thus more readily detectable. Soft failures can take different forms such as a fixed scalar, a fixed bias, a drift, or intermittent spikes. Among these failures, fixed bias will be investigated although the proposed approach can be applied to time-varying soft failures as well.

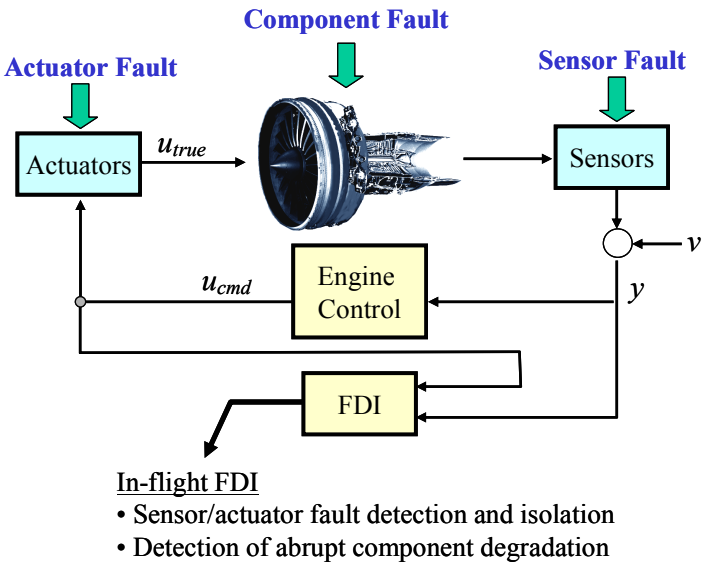

Figure 2. Propulsion System with Fault Detection and Isolation Logic

In the development of the FDI logic, it is assumed that only one of the sensors or actuators will fail at a time. Multiple sequential and multiple simultaneous failures are not addressed in this paper. The likelihood of multiple simultaneous failures is considered to be very low. To handle multiple sequential failures, a hierarchical fault isolation structure, as demonstrated by Menke et al.[10], must be added to the proposed FDI logic.

Component Performance Analysis

The proposed FDI logic uses the Kalman filter approach in order to estimate the state variables, health parameters, and engine output values from a given set of sensor measurements and control commands. A linear model under consideration is represented by the following state-space equations:

$$\begin{aligned} \dot{x} &= Ax + Lh + Bu_{cmd} \\ y &= Cx + Mh + Du_{cmd} + v \end{aligned} \tag{1}$$

where the vectors x, h, and u_{cmd} represent state variables, health parameters, and control commands, respectively. The sensor measurement vector, y, is corrupted by the sensor noise vector, v. The matrices A, B, C, D, L, and M have appropriate dimensions. The influence of the health parameters on an engine is similar to that of the actuation variables; they set the operating condition of an engine. However, unlike the actuation variables, they are not deterministic in nature and must be estimated in order to detect component faults. In the Kalman filter problem setup, the engine state vector is augmented with health parameters as follows[22]:

$$\begin{aligned} \dot{\widetilde{x}} &= \widetilde{A}\widetilde{x} + \widetilde{B}u_{cmd} + w \\ y &= \widetilde{C}\widetilde{x} + Du_{cmd} + v \end{aligned} \tag{2}$$

where

$$\widetilde{x} = \begin{bmatrix} x \\ h \end{bmatrix},\ \widetilde{A} = \begin{bmatrix} A & L \\ 0 & 0 \end{bmatrix},\ \widetilde{B} = \begin{bmatrix} B \\ 0 \end{bmatrix},\ \widetilde{C} = \begin{bmatrix} C & M \end{bmatrix}$$

and w and v are the process and sensor noise, respectively. They are uncorrelated, white noise with the following covariance matrices:

$$\begin{aligned} E\left[w(t+\tau)w^T(t)\right] &= Q\delta(\tau) \\ E\left[v(t+\tau)v^T(t)\right] &= R\delta(\tau) \end{aligned} \tag{3}$$

Kalman filter has the following structure:

$$\begin{aligned} \dot{\widetilde{x}}_e &= \widetilde{A}\widetilde{x}_e + \widetilde{B}u_{cmd} + K(y - y_e) \\ y_e &= \widetilde{C}\widetilde{x}_e + Du_{cmd} \\ K &= P\widetilde{C}^T R^{-1} \end{aligned} \tag{4}$$

where $\widetilde{x}_e$ and y_e are the estimates of the augmented state vector and sensor measurements, respectively, and K is a Kalman gain matrix. The matrix P is the solution of the following steady-state Riccati equation:

$$\widetilde{A}P + P\widetilde{A}^T - P\widetilde{C}^T R^{-1}\widetilde{C}P + Q = 0 \tag{5}$$

In general, the matrix R is derived from available sensor noise characteristic data while the matrix Q is tuned for obtaining a desired Kalman gain. In order for the Kalman filter to converge, the matrix pair $(\widetilde{A}, \widetilde{C})$ must be observable. Moreover, the current problem setup requires the number of health parameters in the augmented state vector to be less than or equal to the number of sensor measurements.[23] The above state-augmented approach is used for designing a bank of Kalman filters for sensor and actuator FDI.

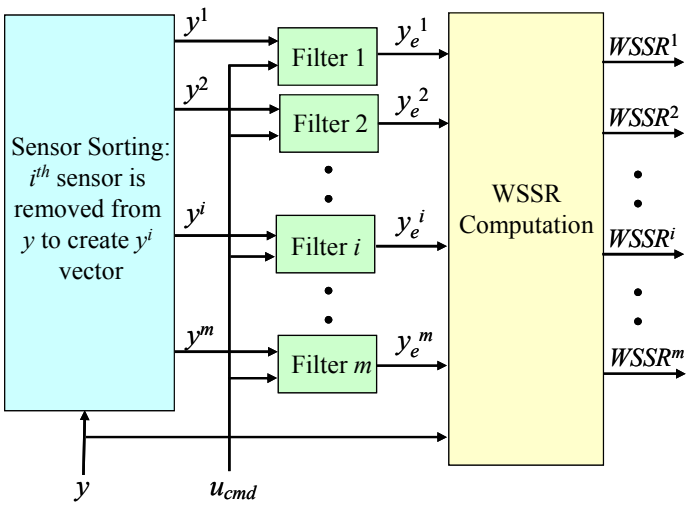

Figure 3. Structure of Bank of Kalman Filters

Sensor Fault Detection

The structure for sensor FDI using a bank of Kalman filters is shown in Figure 3. The bank of Kalman filters contains m Kalman filters where m is the number of sensors being monitored. Each filter estimates the augmented state vector given in Equation (2) using (m-1) sensors. The sensor which is not used by a particular filter is the one being monitored by that filter for fault detection. For instance, the i^{th} filter uses the sensor subset y^i that excludes the i^{th} sensor, where i is an integer from 1 to m. Thus, filter #1 uses all sensors except sensor #1, filter #2 uses all sensors except sensor #2, and so on. In the event that sensor #1 is faulty, all filters will use corrupted measurements, except for filter #1. Consequently, filter #1 is able to estimate the augmented state vector from fault-free sensor measurements, whereas the estimates of the remaining filters are distorted by the fault in sensor #1.

After the estimation of augmented state variables, the sensor measurement estimates are constructed as described in Equation (4). In order to evaluate the accuracy of the state estimation, the following residual vector is generated for each filter:

$$e^i = y_e^i - y^i \tag{6}$$

From this residual, a weighted sum of squared residual (WSSR) is computed:

$$WSSR^i = W_r^i (e^i)^T (\Sigma^i)^{-1} e^i \tag{7}$$

where

$$\Sigma^i = diag[\sigma^i]^2 \tag{8}$$

The vector σ^i represents the standard deviations of the i^{th} sensor-subset, and it normalizes the residual vector. The additional weight W_r is a scalar, and it is selected so that the value of the WSSR signal will be less than a given threshold under the normal condition where all sensors are fault free. The scalar W_r is a tuning parameter that influences the FDI performance. It is desirable to see an obvious increase in the WSSR signal when a sensor is faulty. If the weight W_r is too small, the increase in WSSR will not be observed, causing missed detections. On the other hand, if this scalar is too large, the WSSR signal will be too sensitive to sensor noise and modeling uncertainty and may generate false alarms. The fault indicator signal (i.e., WSSR) will be compared against the detection threshold in order to detect a sensor fault.

Actuator Fault Detection

Actuator FDI is more challenging than sensor FDI in model-based estimation approaches. In the general Kalman filter approach, it is assumed that the actuators are properly configured to the positions that a control system demands, thus any engine responses to actuator perturbations are cancelled out in the estimation loop. However, if a large discrepancy between commanded and true actuator positions does exist due to an actuator fault, it can result in significant state estimation errors. In this paper, an actuator fault is modeled as a bias, which results in inconsistency between an actuator command used as a Kalman filter input and a true actuator position under which the engine is operating.

To account for a potential bias, the following linear model is used in the actuator FDI design approach:

$$\begin{aligned} \dot{x} &= Ax + Lh + B(u_{cmd} + b) \\ y &= Cx + Mh + D(u_{cmd} + b) + v \end{aligned} \tag{9}$$

Equation (9) shows the actuator bias vector b added to the actuator command inputs. Equation (9) can easily be modified such that the bias vector is incorporated in the actuator outputs (See Appendix).

A bank of Kalman filters is also applied for the actuator FDI though its structure will be different from that of the sensor FDI. Unlike the sensor FDI approach where each filter excludes one sensor from the sensor suite, each filter in the actuator FDI will use all m sensors and estimate an augmented state vector, which includes a potential actuator bias. Similar to the sensor FDI approach, the engine state variables in Equation (9) are augmented with health parameters and, in addition, one actuator bias. For bias estimation of the k^{th} actuator, the following model equation is used:

$$\begin{aligned} \dot{\tilde{x}}^k &= \tilde{A}^k \tilde{x}^k + \tilde{B} u_{cmd} + w \\ y^k &= \tilde{C}^k \tilde{x}^k + D u_{cmd} + v \end{aligned} \tag{10}$$

where

$$\tilde{x}^k = \begin{bmatrix} x \\ h \\ b_k \end{bmatrix}, \ \tilde{A}^k = \begin{bmatrix} A & L & B_k \\ 0 & 0 & 0 \\ 0 & 0 & 0 \end{bmatrix}, \ \tilde{B} = \begin{bmatrix} B \\ 0 \\ 0 \end{bmatrix}, \ \tilde{C}^k = \begin{bmatrix} C & M & D_k \end{bmatrix}$$

and k is an integer from 1 to p, where p is the number of actuators. The scalar b_k is a bias in the k^{th} actuator, and the vectors B_k and D_k are the k^{th} columns of B and D matrices, respectively. Based on the above state-space structure, a Kalman filter for each actuator is designed using Equations (3) through (5).

After the estimation of the augmented state variables and sensor measurements, a fault indicator signal is generated for each filter similar to the sensor FDI approach. The residual signal of the $(m+k)^{th}$ filter, where m is the number of sensors, is given as:

$$e^{m+k} = y_e^k - y \tag{11}$$

where the vector y_e^k is the sensor estimates generated by the $(m+k)^{th}$ filter. From this signal, the following weighted sum of squared residual (WSSR) is generated:

$$WSSR^{m+k} = V_r{}^k (e^{m+k})^T (\Sigma)^{-1} e^{m+k} \tag{12}$$

where

$$\Sigma = diag[\sigma]^2 \tag{13}$$

The vector σ is the noise standard deviation, and the scalar V_r is a weighting parameter used for the FDI performance trade off. The fault indicator signal (i.e., WSSR) in Equation (12) will be compared against a given detection threshold in order to detect an actuator fault. When an actuator is biased, all filters use corrupted information, however, the one filter with the correct hypothesis is able to accommodate it. Therefore, this particular filter will maintain a low residual value and consequently can be isolated from the rest of the filters.

Integration of Bank of Kalman Filters with Fault Isolation Logic

The overall architecture of the FDI system is shown in Figure 4. The functionality of the bank of Kalman filters with an augmented state vector is summarized as follows.

1) When there is no sensor or actuator fault, with or without component faults, all Kalman filters should retain low fault indicator signals, indicating there is no sensor/actuator fault, and should generate accurate health parameter estimates.

2) When one of the sensors or actuators failed, with or without component faults, only the one filter with the correct hypothesis should generate a low fault indicator signal and accurate health parameter estimates.

The fault indicator signals generated by the above approach must be further processed in order to identify a fault. The FDI process can be completed by integrating the bank of Kalman filters with fault isolation logic as shown in Figure 4. In general, fault isolation logic is constructed from detection thresholds and decision rules. The decision rules check for fault indicator signal violation of the pre-established

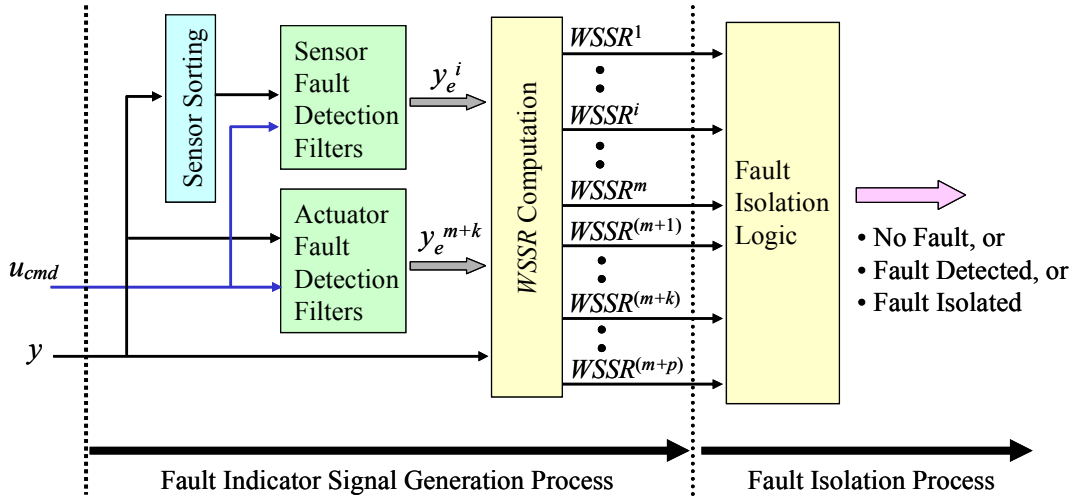

Figure 4. FDI System Architecture

detection thresholds. If the necessary rules for the existence of a fault are satisfied, then the fault isolation logic declares a fault. Fault isolation is achieved if a fault is declared for all the fault indicator signals except for the one corresponding to a correct fault hypothesis. The development of fault isolation logic is application-dependent. An example will be given in the following section where the FDI design methodology is applied to the aircraft engine model.

5.0 Application of FDI Methodology to the Aircraft Engine

In this section, the FDI design methodology is applied to the aircraft engine model described in Section 3.0. An assumption made for this application problem is discussed followed by a discussion of various design parameters for the FDI system and a description of the fault isolation logic development.

Application Specific Engine Model Assumption

As shown in Table 1, the aircraft engine model has three state variables, 10 health parameters, three actuators, and eight sensors. The standard deviation of the sensor noise vector used in this study is shown in Table 2. These numbers are rough estimates derived from Lu et al.[24] Information regarding sensor accuracy can be also found in Pinelli et al.[25]

Table 2. Sensor Noise Standard Deviation in % of the Nominal Engine Trim Values

Sensor	XN2	XN25	T27D	T56	PS15	P27	PS3	PS56
σ	0.25	0.25	0.5	0.5	0.5	0.5	0.5	0.5

An assumption is made in this application problem. It is assumed that the first four health parameters (FAN and BST efficiency and flow capacity scalars) in Table 1 are sufficient to represent component faults of interest during a flight. As discussed in Section 3.0, the health parameters deviate from the initial healthy baseline condition over time due to gradual degradation (baseline degradation) and possibly abrupt degradation (fault). The focus of the current research is the detection of component faults. The four health parameters are used to represent an abrupt, moderate degradation due to foreign object damage (FOD), as done by Kerr et al.[26] The detection of such faults is achieved by accurately estimating those selected health parameters. The four health parameters are included in the augmented state vector and estimated as described by Equations (2) through (5). The selection of the four health parameters was based upon their correlation to FOD events and the relative likelihood of an engine experiencing FOD versus other possible abrupt component degradations during a flight. If alternative faults are known to be more probable, the FDI system can be re-designed using those health parameters which correlate to the faults of interest. The design constraint is that the selected health parameters must be observable through the given sensor suite.

Design Parameters for the FDI System

Some of the design parameters, such as sensor and process noise covariance matrices and residual weighting factors, are specified in this section. The Kalman filter covariance matrices for the i^{th} sensor are given as:

$$R^{i}{}_{sensor} = \Sigma^{i}$$
$$Q_{sensor} = diag\begin{bmatrix} 0.02 & 0.02 & 0.02 & 0.03 & 0.03 & 0.03 & 0.03 \end{bmatrix} \tilde{x}_{trim}$$

where Σ^{i} is the noise weighting factor (Equation 8), and $\tilde{x}_{trim}$ is the trim values of the augmented state vector (Equation 2) at the nominal baseline condition. Since all eight sensor FDI filters are estimating the same augmented state vector, the process noise covariance is the same for all filters.

The Kalman filter covariance matrices for the k^{th} actuator are given as:

$$R_{actuator} = \Sigma$$
$$Q^{k}{}_{actuator} = diag\begin{bmatrix} 0.02 & 0.02 & 0.02 & 0.03 & 0.03 & 0.03 & 0.03 & 0.02 \end{bmatrix} \tilde{x}^{k}_{trim}$$

where Σ is the noise weighting factor (Equation 13), and $\tilde{x}^{k}_{trim}$ is the trim values of the augmented state vector (Equation 10) at the nominal baseline condition. Since all three actuator FDI filters are using the same eight sensors, the measurement noise covariance is the same for all filters.

Initially, for all 11 FDI filters, the same fraction (0.02) of the trim values was used for all augmented state variables in the process noise covariance matrices. The intent was to simplify the design process by not using different weights for each augmented state variable. After some investigation, the weight for the health parameters was increased to 0.03 in order to improve the robustness of health parameter estimation.

The residual weighting factors for the sensor (Equations 7) and actuator (Equations 12) FDI filters are:

$$W_r^{\,i} = 1/7 \qquad \text{where} \quad i = 1 \sim m$$
$$V_r^{\,k} = 1/8 \qquad \text{where} \quad k = 1 \sim p$$

With the above residual weights, the mean values of the fault indicator signals of all 11 Kalman filters are slightly below one when there is no fault in the sensors or actuators. Although the same weighting factors were used for both the sensor and actuator sets, they can be varied for performance trade off.

Development of Fault Isolation Logic

In order to isolate a fault using the bank of Kalman filters developed in the previous sections, fault isolation logic must be developed. This decision-making logic is discussed in this section in the context of a simulated example. Consider an example in which the fault indicator signal generation process in Figure 4 is applied to the nonlinear engine simulation for a scenario where all the sensors and actuators remain fault free. Figure 5 shows the actual sensor measurement responses and their estimates produced by the 11 FDI filters. Figure 6 shows the actual health parameter perturbations and the estimates produced by the 11 FDI filters. Figure 7 shows the fault indicator signals (WSSR) of the 11 FDI filters; these signals have been filtered through a low-pass filter with a cutoff frequency of 1.0 rad/sec. It can be observed that the noise in the sensor measurements is quite significant, causing large variations in health parameter estimates and fault indicator signals.

Two factors that are of main concern in developing the fault isolation logic are false alarms and missed detections. Reducing one of these factors often causes an increase in the other. To illustrate how the isolation logic affects false alarms and missed detections, assume that, in the current case, a fault is declared for an FDI filter when the corresponding fault indicator signal exceeds a given detection threshold. If the detection threshold is set at the value of one, all of the fault indicator signals in Figure 7 exceed the detection threshold; therefore multiple false alarms would have occurred. To avoid such false alarms, two options are possible: 1) increase the detection threshold value, or 2) smooth the fault indicator signals by modifying the bandwidth of the low-pass filter. Both options, however, may cause missed detections. A fault may result in a shift in the mean value of some fault indicator signals without any spike-like responses. In such a case, a failure scenario will go undetected until the magnitude of the fault becomes severe enough to reach the higher threshold. Also, reducing the bandwidth of the low-pass filter will eliminate any spike-like fault signatures in the fault indicator signals, making such failures more difficult to detect.

In the current study, a modified approach for fault isolation is developed in order to reduce false alarms and missed detections as much as possible. First of all, the fault indicator signals of all 11 FDI filters are averaged over non-overlapping, ten-second intervals. For sensor FDI filters, two thresholds are used: the first threshold is set at the value of one, and the second is set at the value of two. A fault is declared if the ten-second averaged fault indicator signal exceeds the first threshold three consecutive times, or if the non-averaged fault signal exceeds the second threshold. The first rule (using the averaged signal) addresses a mean value shift of the fault indicator signal that is sustained. This rule results in a minimum fault identification time of 30 seconds. The second rule (using the non-averaged signal) obviously takes into account spike-like fault signatures. The second threshold is set high enough so that sensor noise or modeling uncertainty will not cause the fault indicator signal to exceed it.

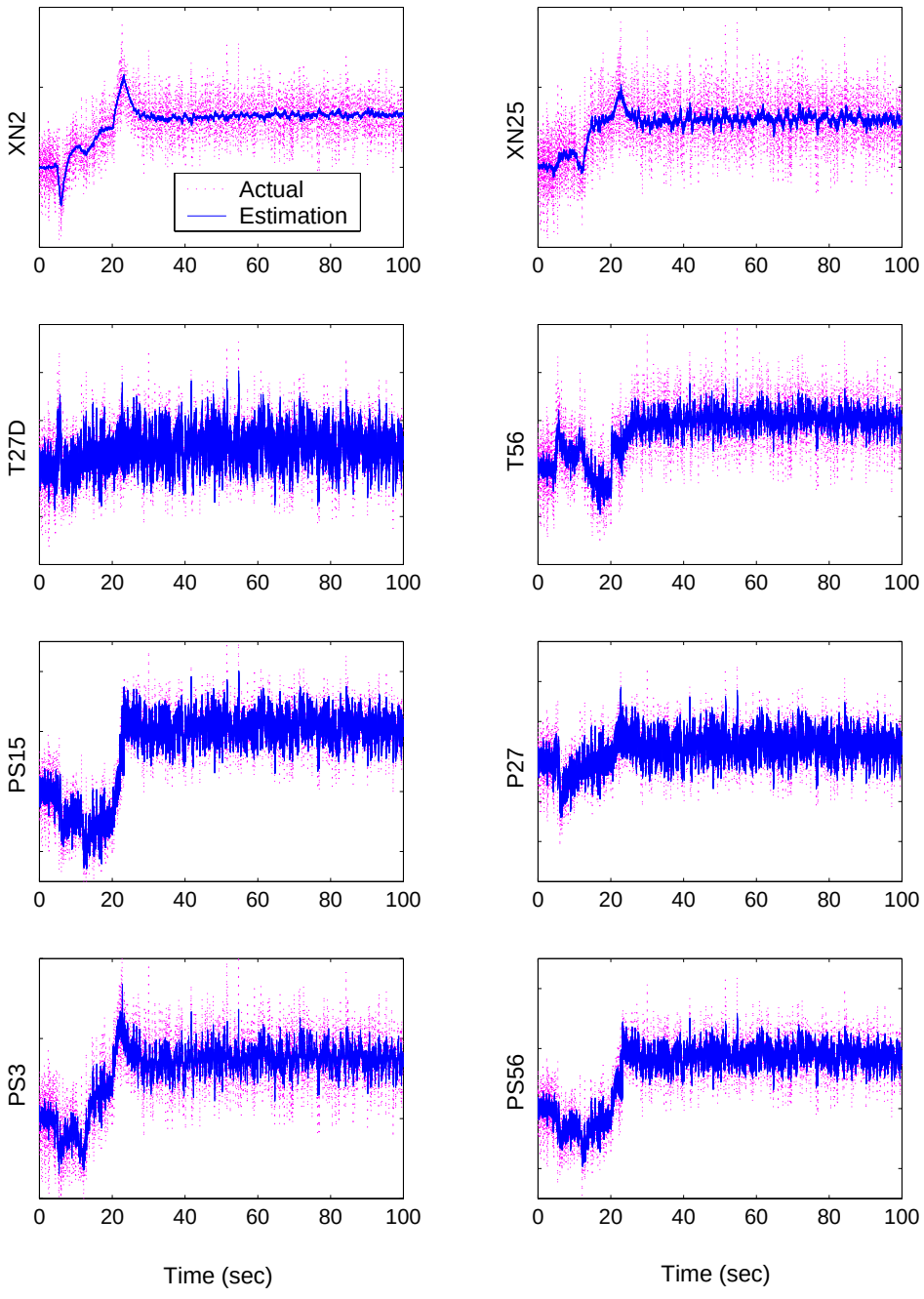

Figure 5. Actual and Estimated Measurement Responses of 11 FDI Filters

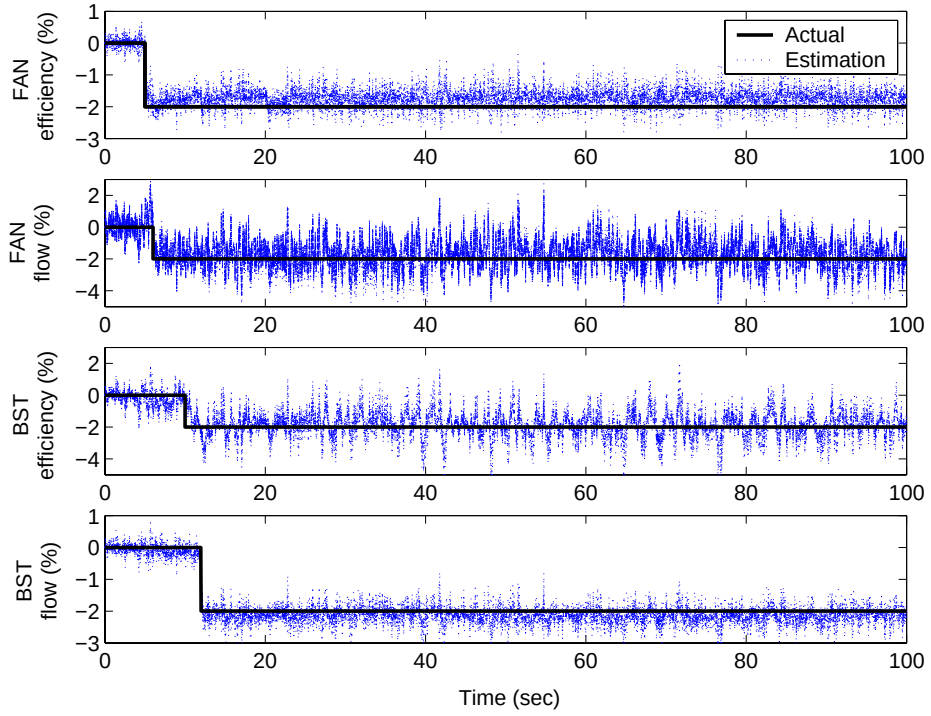

Figure 6. Actual and Estimated Health Parameters of 11 FDI Filters

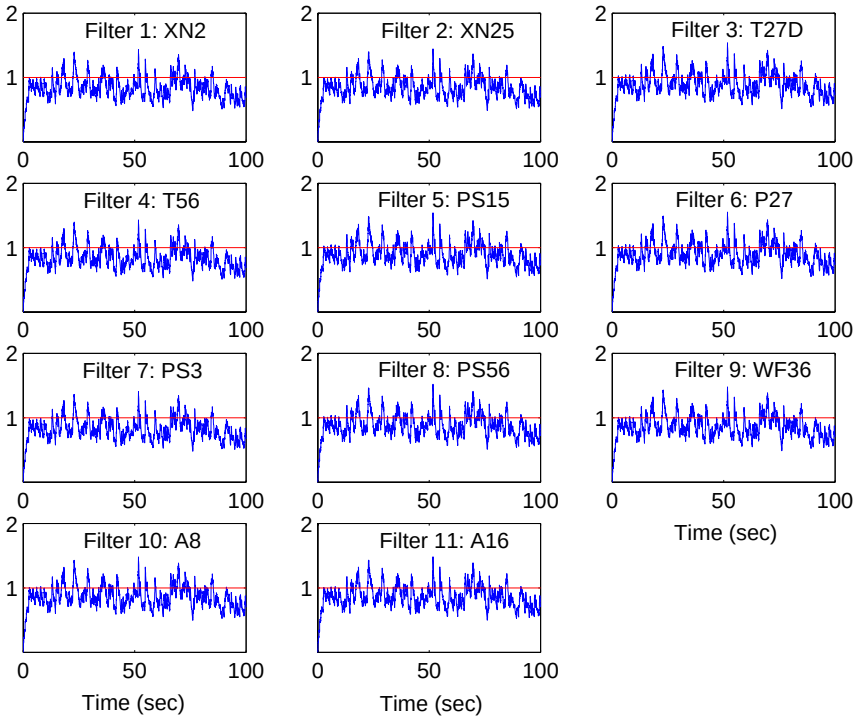

Figure 7. Fault Indicator Signal Responses of 11 FDI Filters

For actuator FDI filters, only one threshold, set at the value of one, is used. A fault is declared if the ten-second averaged fault indicator signal exceeds the threshold four consecutive times. The reason for applying a different rule for actuator failures is as follows. For actuator FDI, the response of the "correct" Kalman filter is influenced by an actuator bias, whereas a sensor bias does not influence the response of the "correct" filter for sensor FDI. When an actuator is biased, the actuator position estimated by the "correct" Kalman filter initially follows the control command, indicating that there is no bias. After going through this initial error phase, the estimated position starts converging to the true actuator position. This initial estimation error can be huge depending on the bias magnitude. Therefore, spike-like signatures, which could be generated by both "correct" and "wrong" Kalman filters, cannot be used as an actuator fault indicator. Moreover, the initial estimation error transient of the "correct" Kalman filter may result in high residuals which persist for longer periods than in the sensor FDI case. To account for this fact, the detection threshold must be violated four consecutive times before declaring a fault, instead of three times as for the sensor FDI.

The sensor and actuator FDI decision process is shown in Figure 8. Fault isolation is successfully achieved when the isolation logic detects a fault in all FDI filters except for the one "correct" filter. If a "wrong" filter is isolated, it is considered a false alarm. If the isolation logic detects a fault in at least one filter, but multiple filters indicate no-fault, it means that a fault was detected but not isolated. FDI performance depends on the decision rules and the values of the detection thresholds. They are adjusted by the designer in order to meet the desired system performance requirements.

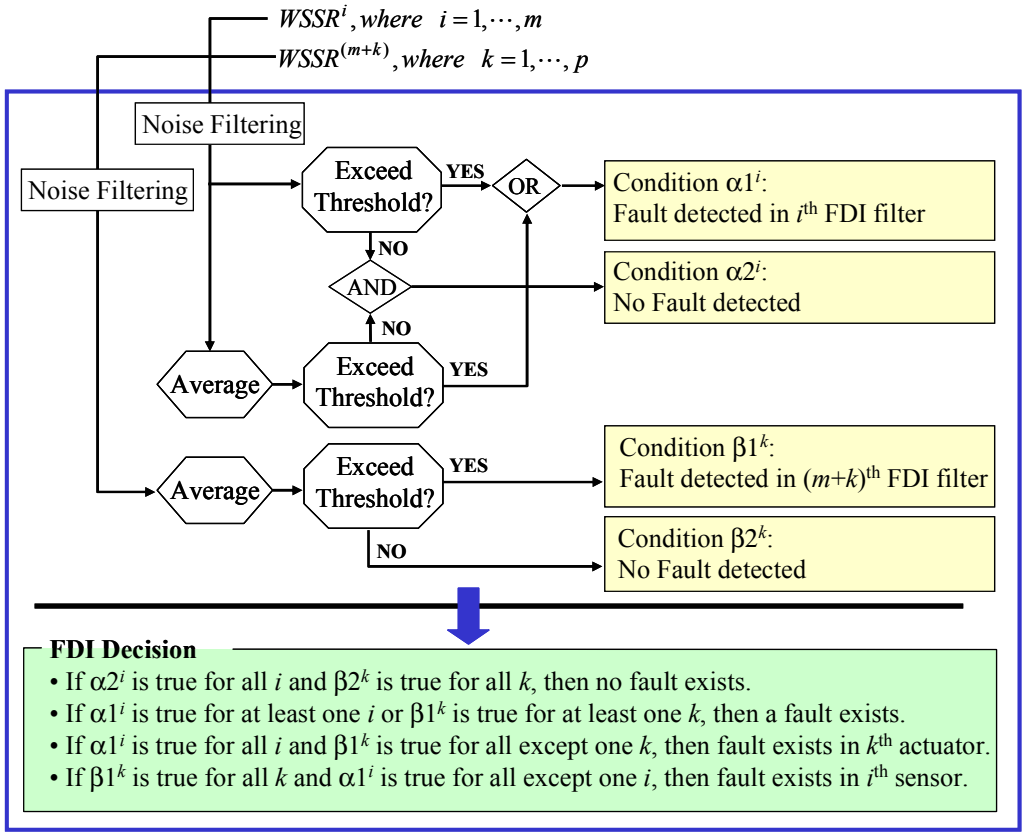

Figure 8. FDI Decision Process

6.0 Integration of the FDI System with the Steady-State Condition Monitoring System

In the real engine environment, a mismatch in the health condition between an operational (aging) engine and the "nominal" engine model used by the FDI system almost always exists. As discussed in Section 3.0, gradual degradation due to aging is referred to as baseline degradation and is represented by deviations in all 10 health parameters from the healthy baseline condition. If the baseline degradation is not accounted for in the FDI design, the baseline mismatch will impact the FDI performance. To demonstrate this impact, three baseline conditions shown in Table 3 are considered. The effects of baseline mismatch on the FDI performance are shown in Table 4, where the FDI system designed at the healthy baseline condition is applied to the nonlinear engine simulation at three baseline conditions in Table 3.

Table 3. Baseline Degradations in % from the Nominal Baseline Condition

	Condition 1 Nominal (Healthy)	Condition 2 Moderate degradation	Condition 3 Severe degradation
FAN efficiency	0	-1.00	-1.80
FAN flow	0	-1.25	-2.20
BST efficiency	0	-1.00	-2.00
BST flow	0	-1.10	-2.20
HPC efficiency	0	-1.00	-1.50
HPC flow	0	-0.80	-1.20
HPT efficiency	0	-1.00	-2.00
HPT flow	0	0.75	1.50
LPT efficiency	0	-1.00	-1.20
LPT flow	0	1.65	2.00

Table 4 shows the estimation performance of the 11 FDI filters. The engine simulation was run at a steady-state cruise point over 100 seconds (no control perturbations) without any sensor, actuator, or component faults. All estimation values were averaged over 100 seconds. Note that the sensor and actuator bias estimates are also given. As expected, the deviations in all 10 health parameters (baseline degradation) for conditions #2 and #3 are incorrectly attributed, or "smeared," to the four health parameters being estimated, resulting in unacceptable health estimation. A similar result was observed in real engine testing conducted by Luppold et al.[27] Moreover, the overall sensor/actuator FDI performance varied apparently with the baseline degradation: none of the FDI filters caused the fault isolation logic to declare a fault for baseline condition #1, whereas all 11 FDI filters resulted in declaring a fault for baseline condition #3. For baseline condition #2, six out of 11 FDI filters resulted in declareing a fault. The FDI filters which generated false alarms are highlighted in Table 4. This example demonstrates the sensitivity of the FDI system, which is designed based on a healthy engine, to the baseline degradation of aging engines.

Table 4. Estimation Performance of the FDI System at Steady-State Cruise Condition
(FDI system is designed at baseline condition #1.)

		Average Estimation				
FDI Filter #	Nonlinear Baseline Condition	Bias (% of trim)	FAN Efficiency (%)	FAN Flow (%)	BST Efficiency (%)	BST Flow (%)
1 (XN2)	1	-0.03	-0.05	-0.11	0.09	0.05
	2	-3.06	-8.32	-10.36	4.63	4.92
	3	-3.95	-11.45	-13.98	1.37	6.13
2 (XN25)	1	0.00	-0.01	-0.02	0.01	0.01
	2	0.16	-2.56	-1.92	-3.33	1.21
	3	0.34	-3.62	-3.03	-8.94	1.37
3 (T27D)	1	0.00	0.00	-0.02	0.01	0.01
	2	-0.59	-3.33	-1.02	-3.26	0.51
	3	-0.88	-5.00	-1.67	-8.85	0.28
4 (T56)	1	-0.01	-0.01	-0.02	0.01	0.01
	2	0.21	-2.80	-1.84	-2.93	1.09
	3	0.20	-4.18	-2.86	-8.77	1.12
5 (PS15)	1	0.00	0.00	-0.02	0.03	0.01
	2	-0.56	-2.69	-1.30	-1.81	2.02
	3	-0.94	-3.91	-1.96	-6.87	2.60
6 (P27)	1	0.00	0.00	-0.02	0.00	0.01
	2	0.75	-4.58	-2.91	0.59	2.57
	3	1.26	-7.12	-4.64	-2.62	3.56
7 (PS3)	1	0.00	0.00	-0.02	0.02	0.01
	2	-0.29	-2.77	-1.91	-3.29	0.89
	3	-0.64	-4.01	-3.00	-9.35	0.55
8 (PS56)	1	0.00	0.00	-0.02	0.02	0.01
	2	0.33	-2.93	-2.08	-3.86	0.88
	3	0.60	-4.34	-3.28	-10.23	0.67
9 (WF36)	1	0.02	0.00	-0.01	0.03	0.01
	2	0.36	-2.75	-1.71	-3.02	1.23
	3	0.42	-4.11	-2.71	-8.80	1.27
10 (A8)	1	-0.01	0.00	-0.01	0.04	0.03
	2	0.47	-2.90	-2.55	-4.68	-0.12
	3	1.02	-4.29	-4.36	-12.20	-1.56
11 (A16)	1	-0.01	0.00	-0.02	0.02	0.01
	2	-2.01	-2.62	-1.47	-2.83	1.54
	3	-3.07	-3.87	-2.29	-8.43	1.77

Robustness Improvement Through the System Integration

The loss of FDI performance due to aging effects can be partially recovered by modifying any of the following three parts of the FDI system shown in Figure 9: 1) Trim Value Data, 2) Bank of Kalman Filters, and 3) Fault Isolation Logic.

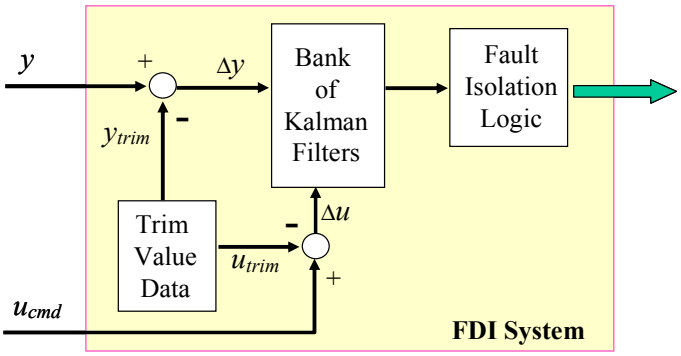

Figure 9. Structure of the FDI System

The trim value data contains sensor and actuator steady-state values at a trim condition where the bank of Kalman filters is designed. (Note that the actuator trim condition is currently independent of baseline degradation since the FDI system is running in an open-loop manner.) As the baseline degradation worsens, the difference in the steady-state values at the trim point between the degraded and healthy engines increases, causing a loss of FDI performance. If the trim value data is updated to account for baseline degradation, the initial steady-state estimation errors can be eliminated. In this approach, a mismatch between the dynamics of the operational engine and the nominal model used by the FDI system may still exist. A more involved option for reducing the estimation errors is to update the bank of Kalman filters based on the baseline degradation. After updating the trim value data, a linear model can be generated at the corresponding trim condition. By designing a bank of Kalman filters based on this linear model, both the initial steady-state condition and the dynamics of the FDI system will match with those of the operational engine. The ease with which such linear model generation can be achieved is key for making this approach practical. Another option for regaining the lost FDI performance is to modify the fault isolation logic. The difference in the initial steady-state values between the operational engine and the nominal trim value data causes an increase in the steady-state values of the fault indicator signals. By simply setting the threshold at a higher value, a false alarm can be avoided. However, this approach results in conservative performance when the operational engine is healthy. Among the three options discussed above, the first two options (updating the trim value data and updating the bank of Kalman filters) will be evaluated in the following section. It is considered that these updates are done by the steady-state condition monitoring system discussed in Section 3.0.

7.0 Performance Evaluation of the FDI System

The performance of the FDI system is evaluated in this section by applying it to the nonlinear engine simulation trimmed at a cruise operating point. The FDI performance is evaluated based on the minimum bias magnitude which can be isolated, and the accuracy of health parameter estimates. Multiple scenarios are considered to ensure that the FDI system does not identify any component faults as a sensor or actuator fault. To capture a range of expected component faults, the eight scenarios, shown in Table 5 with health parameter and control command perturbation magnitude and injection time information, are investigated. In the simulation, these perturbations are injected as step changes at the specified time. The perturbations in the four health parameters represent abrupt component degradation due to a FOD event. Since field data indicating actual component degradation profiles due to FOD was not available, the magnitudes and injection times were selected arbitrarily. Likewise, control command perturbations were

selected arbitrarily to represent operation around the fixed operating point. As shown in Table 5, multiple health parameters are perturbed in order to introduce the nonlinear effects on the engine simulation outputs. The control command perturbations disturb the engine operating point; however, they must not cause a false alarm. Given these perturbations, the nonlinear engine simulation generates the sensor measurements, which are then used by the FDI system.

Table 5. Engine Operating Scenarios for Evaluation of the FDI System at Cruise

Scenario #	Perturbation Description (magnitude and step time)						
	FAN efficiency	FAN flow	BST efficiency	BST flow	WF36	A8	A16
1	0	0	0	0	0	0	0
2	0	0	0	0	2% at 5 sec	-1% at 8 sec	-3% at 7 sec
3	-1% at 5 sec	-1% at 6 sec	-1% at 10 sec	-1% at 12 sec	0	0	0
4	-1% at 5 sec	-1% at 6 sec	-1% at 10 sec	-1% at 12 sec	2% at 20 sec	-1% at 23 sec	-3% at 22 sec
5	-2% at 5 sec	-2% at 6 sec	-2% at 10 sec	-2% at 12 sec	0	0	0
6	-2% at 5 sec	-2% at 6 sec	-2% at 10 sec	-2% at 12 sec	2% at 20 sec	-1% at 23 sec	-3% at 22 sec
7	-3% at 5 sec	-3% at 6 sec	-3% at 10 sec	-3% at 12 sec	0	0	0
8	-3% at 5 sec	-3% at 6 sec	-3% at 10 sec	-3% at 12 sec	2% at 20 sec	-1% at 23 sec	-3% at 22 sec

Performance Evaluation Results

The performance of the FDI system is evaluated by applying it to the nonlinear simulation for the eight scenarios in Table 5. For each scenario, the nonlinear simulation is executed for 100 seconds at the three baseline conditions shown in Table 3. The abrupt health parameter perturbations in Table 5 are deviations from the baseline conditions in Table 3. Therefore, a 3% reduction in FAN flow capacity (Scenarios 7 and 8) for engine baseline #3 (Table 3) means 5.2% degradation in total. In the cases where the FDI system is applied to the nonlinear simulation at baseline conditions #2 and #3, two parts of the FDI system, 1) trim value data and 2) bank of Kalman filters, are updated based on the baseline degradation, and the benefits of this update is assessed.

A sensor or actuator bias is injected as a step change when the simulation time reaches 30 seconds. As previously mentioned, the FDI performance is evaluated based on the minimum magnitude of the sensor/actuator bias which can be isolated, and the accuracy of health parameter estimates. The smaller the minimum bias that can be isolated, the better the performance of the FDI system is considered to be. However, if the minimum isolated bias becomes too small relative to noise, the assumption that one sensor or actuator may be biased at a time may no longer hold since multiple sensors and actuators may have small biases in the real engine environment. Therefore, it is undesirable to have an FDI system which is overly sensitive to small sensor or actuator bias. For health parameter estimation, the performance is considered acceptable if the average estimation error (the difference between true and estimated values) is less than 0.5%.

1) Nominal Performance: Baseline Condition #1

In this section, the FDI system designed based on baseline condition #1 is applied to the nonlinear simulation at baseline condition #1. Prior to determining the minimum bias that can be isolated, it must be verified that the FDI system would not generate a false alarm when there is no sensor or actuator fault. This was confirmed for all eight simulation scenarios.

Table 6 shows the results of the FDI performance evaluation for the positive bias case. For each of the eight simulation scenarios, a bias was injected into one of the sensors or actuators, and then the bias with the smallest magnitude that could be isolated by the FDI system was determined. The isolated minimum positive bias is in % of trim value of the nominal baseline condition. It is desirable to normalize the bias by full-scale values in addition to trim values. However, full-scale values for this engine model are currently not available. The numbers in parentheses indicate the Euclidian distance (square root of sum of squares) of four health parameter estimation errors, each of which was averaged over the last 50 seconds of the simulation. The entries that correspond to cases where at least one health parameter estimation error was larger than or equal to 0.5% are shaded. It should be noted that the health parameter estimation accuracy of each of the eight sensor FDI filters is independent of a bias in the corresponding sensor. The FDI system was successfully able to detect and isolate the fault in all sensors and actuators for all scenarios (88 cases) without generating a false alarm.

From Table 6, it is observed that the magnitude of the minimum isolated bias for individual sensors and actuators varies slightly with the simulation scenario. However, apparent variations in bias magnitude can be observed between different sensors and actuators. For instance, the bias in the XN25 sensor can be isolated at low magnitude while the minimum bias that can be isolated in the A16 actuator is quite large. The performance variations among the FDI filters are considered to be mainly due to the uniqueness of the information provided by the sensors and actuators. During the course of the performance evaluation, it was found that the following pairs of FDI filters were difficult to isolate from each other: T56 and WF36, PS15 and A16, and PS56 and A8. It should be note that these sensors (T56, PS15, PS56) are directly influenced by the corresponding actuators (WF36, A16, A8). Particularly, in the cases where either PS15 or A16 is biased, the two FDI filters focused on these parameters retain low fault indicator signals until the bias magnitude becomes very large (see Table 6). A possible approach to handle such a problem is to utilize additional information, besides the sensor estimation error, in the fault decision-making process. Although two filters generate small sensor estimation errors, it was found that the "wrong" filter usually generates health parameter estimates that are beyond the expected linear range. For instance, in scenario 1, all filters except for PS15 and A16 filters exceed the detection threshold when the bias in PS15 is 1.5%. Although the two filters retain low residuals, the A16 filter generates a health parameter estimate above 5.0%, which is considered well beyond the linear range. By putting some bounds on health parameter estimates, any filter which generates estimated values beyond those bounds could be penalized when the fault indicator signal is computed.

The difficulty of accurately estimating health parameters increases as the magnitude of the step perturbations in these parameters (component fault) increases. For most of the FDI filters, the health parameter estimates are acceptable except for scenario 7. Scenario 7 can be considered a borderline case where the estimation performance of the FDI filters starts to deviate from the acceptable level. FDI filter #1 (XN2) generates at least one health parameter estimation error above 0.5% in scenarios 6 and 8. The low-spool speed provides essential information for estimating health parameters; therefore the cases where the XN2 sensor is biased are very challenging in terms of obtaining accurate estimation of health parameters.

Table 7 shows the results of the FDI performance evaluation for the negative bias case. The overall results are very similar to the positive bias case though some minor differences in the bias magnitude and the accuracy of health parameter estimation are observed.

Table 6. Performance of the FDI System Applied to Nonlinear Simulation at Baseline Condition #1, Positive Bias Case

Simulation Scenario #	Isolated Minimum Positive Bias in % of Nominal Trim Value (Euclidian distance of health parameter estimation errors in parentheses)										
	XN2	XN25	T27D	T56	PS15	P27	PS3	PS56	WF36	A8	A16
1	3.3 (0.11)	0.9 (0.01)	1.4 (0.03)	2.8 (0.03)	12.1 (0.07)	3.2 (0.01)	1.4 (0.01)	4.8 (0.05)	2.6 (0.01)	5.6 (0.06)	25.1 (0.02)
2	3.3 (0.23)	1.1 (0.19)	1.3 (0.17)	2.4 (0.19)	12.1 (0.20)	3.9 (0.23)	1.5 (0.16)	4.7 (0.21)	3.2 (0.19)	6.0 (0.19)	32.3 (0.18)
3	3.6 (0.27)	1.1 (0.32)	1.3 (0.34)	2.6 (0.33)	10.2 (0.34)	3.5 (0.32)	1.5 (0.36)	4.2 (0.35)	3.1 (0.34)	5.5 (0.34)	34.9 (0.33)
4	3.5 (0.35)	1.3 (0.21)	1.3 (0.21)	2.9 (0.22)	9.7 (0.21)	3.7 (0.22)	1.3 (0.23)	3.5 (0.25)	3.1 (0.19)	5.3 (0.26)	32.8 (0.18)
5	2.8 (0.49)	0.9 (0.58)	1.2 (0.59)	2.1 (0.59)	9.7 (0.58)	3.9 (0.60)	1.3 (0.58)	3.5 (0.57)	2.4 (0.60)	5.8 (0.62)	25.1 (0.59)
6	2.8 (0.70)	0.9 (0.47)	1.1 (0.47)	2.1 (0.48)	10.1 (0.47)	3.8 (0.53)	1.3 (0.46)	3.5 (0.46)	2.7 (0.46)	5.7 (0.50)	25.6 (0.47)
7	3.4 (0.76)	1.1 (0.77)	1.4 (0.78)	2.6 (0.78)	11.9 (0.76)	3.1 (0.82)	1.4 (0.79)	4.2 (0.80)	2.9 (0.80)	5.9 (0.86)	30.1 (0.77)
8	3.3 (0.86)	1.1 (0.66)	1.3 (0.65)	2.6 (0.66)	11.8 (0.65)	3.1 (0.77)	1.4 (0.66)	4.2 (0.68)	3.0 (0.68)	5.9 (0.71)	30.4 (0.65)

Table 7. Performance of the FDI System Applied to Nonlinear Simulation at Baseline Condition #1, Negative Bias Case

Simulation Scenario #	Isolated Maximum Negative Bias in % of Nominal Trim Value (Euclidian distance of health parameter estimation errors in parentheses)										
	XN2	XN25	T27D	T56	PS15	P27	PS3	PS56	WF36	A8	A16
1	-3.3 (0.11)	-0.9 (0.01)	-1.3 (0.01)	-2.4 (0.01)	-13.8 (0.07)	-3.3 (0.01)	-1.3 (0.05)	-4.3 (0.05)	-2.6 (0.01)	-5.1 (0.06)	-27.6 (0.02)
2	-3.3 (0.23)	-1.1 (0.21)	-1.3 (0.17)	-2.3 (0.18)	-12.5 (0.20)	-3.9 (0.23)	-1.4 (0.16)	-4.6 (0.21)	-2.6 (0.17)	-6.4 (0.21)	-31.5 (0.20)
3	-3.5 (0.26)	-1.0 (0.33)	-1.2 (0.34)	-2.7 (0.36)	-10.2 (0.34)	-3.5 (0.32)	-1.3 (0.34)	-4.2 (0.35)	-2.9 (0.36)	-6.5 (0.35)	-31.6 (0.33)
4	-3.5 (0.34)	-1.2 (0.21)	-1.3 (0.20)	-2.2 (0.24)	-8.9 (0.21)	-3.6 (0.21)	-1.3 (0.22)	-3.6 (0.25)	-2.6 (0.24)	-6.8 (0.28)	-38.0 (0.20)
5	-2.8 (0.49)	-0.9 (0.56)	-1.1 (0.57)	-2.3 (0.56)	-9.7 (0.58)	-3.4 (0.60)	-1.4 (0.59)	-3.4 (0.57)	-2.7 (0.60)	-5.4 (0.61)	-28.6 (0.59)
6	-2.9 (0.70)	-0.9 (0.44)	-1.2 (0.45)	-2.2 (0.45)	-10.3 (0.47)	-3.4 (0.53)	-1.4 (0.48)	-3.4 (0.47)	-2.6 (0.48)	-5.5 (0.50)	-26.5 (0.47)
7	-3.5 (0.76)	-1.0 (0.77)	-1.3 (0.76)	-2.6 (0.76)	-11.2 (0.77)	-3.1 (0.82)	-1.5 (0.78)	-4.3 (0.80)	-3.0 (0.81)	-6.3 (0.86)	-30.9 (0.78)
8	-3.5 (0.86)	-1.0 (0.66)	-1.3 (0.64)	-2.6 (0.65)	-11.3 (0.66)	-3.1 (0.78)	-1.4 (0.67)	-4.3 (0.68)	-2.9 (0.68)	-6.3 (0.71)	-30.5 (0.67)

2) FDI Performance Recovery Through Updating the Trim Value Data

In this section, the FDI system designed based on baseline condition #1 is applied to the nonlinear simulation at baseline conditions #2 and #3. A loss of FDI performance due to baseline mismatch was investigated in Section 6.0. In order to partially recover the FDI performance, the trim value data is updated based on the new baseline condition so that the initial steady-state mismatch is eliminated.

a. Baseline Condition #2

Tables 8 and 9 show the performance evaluation results when the FDI system is applied to the nonlinear simulation at baseline condition #2. Table 8 shows the positive bias case while Table 9 shows the negative bias case. No false alarms were generated on any simulation scenario with sensor/actuator bias (88+88 cases) or without sensor/actuator bias (8 scenarios).

It can be observed that the magnitude of the minimum isolated bias is very close to the previous case, indicating that the loss of sensor/actuator FDI performance due to mismatch in the baseline condition can be recovered by updating the trim value data. However, health parameter estimation accuracy is not recovered. The estimation errors become very large when health parameter step perturbations exceed 2% (scenarios 5 through 8). Although the initial steady-state values were made to match, the new steady-state values after the perturbations do not match because of the difference in the dynamics (specifically, steady-state gain) between the nonlinear simulation and the FDI system. As discussed before, when there is a mismatch in the steady-state condition, the mismatch is "smeared" to the four health parameters being estimated. Thus, the four health parameters may no longer represent the actual health parameters. Instead, they become "tuning" parameters. A Kalman filter tunes these four health parameters so that its sensor estimates will match with the outputs of the nonlinear simulation. To improve the estimation accuracy, it is expected that the bank of Kalman filters must be updated based on the baseline degradation.

Table 8. Performance of the FDI System with Updated Trim Value Data Applied to Nonlinear Simulation at Baseline Condition #2, Positive Bias Case

Simulation Scenario #	Isolated Minimum Positive Bias in % of Nominal Trim Value (Euclidian distance of health parameter estimation errors in parentheses)										
	XN2	XN25	T27D	T56	PS15	P27	PS3	PS56	WF36	A8	A16
1	3.3 (0.11)	0.8 (0.01)	1.4 (0.03)	2.8 (0.03)	12.1 (0.07)	3.2 (0.01)	1.4 (0.01)	4.8 (0.05)	2.6 (0.01)	5.6 (0.06)	25.1 (0.03)
2	3.4 (0.50)	1.2 (0.19)	1.4 (0.20)	2.3 (0.15)	12.5 (0.22)	3.9 (0.23)	1.4 (0.20)	4.6 (0.21)	3.0 (0.23)	6.2 (0.20)	31.0 (0.21)
3	3.6 (0.44)	1.0 (0.56)	1.3 (0.56)	2.2 (0.58)	10.4 (0.59)	3.6 (0.56)	1.3 (0.59)	4.2 (0.58)	3.2 (0.58)	5.8 (0.58)	31.9 (0.56)
4	3.5 (0.25)	1.1 (0.44)	1.3 (0.48)	2.1 (0.47)	9.8 (0.48)	3.7 (0.36)	1.3 (0.49)	4.5 (0.49)	3.0 (0.44)	5.2 (0.45)	32.5 (0.43)
5	3.0 (0.92)	0.9 (1.08)	1.2 (1.09)	2.4 (1.08)	9.1 (1.07)	3.8 (0.99)	1.3 (1.08)	3.8 (1.07)	2.6 (1.10)	5.7 (1.08)	23.8 (1.08)
6	3.0 (0.47)	1.0 (1.00)	1.2 (1.02)	2.3 (1.01)	9.3 (0.98)	3.8 (0.87)	1.3 (0.99)	3.8 (0.98)	2.6 (1.00)	5.9 (0.96)	24.2 (1.01)
7	3.5 (1.39)	1.1 (1.57)	1.2 (1.57)	2.6 (1.55)	11.3 (1.56)	3.1 (1.39)	1.4 (1.58)	4.5 (1.56)	3.1 (1.56)	6.1 (1.56)	34.1 (1.53)
8	3.5 (0.82)	1.1 (1.52)	1.3 (1.54)	2.6 (1.51)	11.5 (1.49)	3.1 (1.31)	1.4 (1.51)	4.3 (1.50)	3.0 (1.50)	6.3 (1.48)	32.7 (1.51)

Table 9. Performance of the FDI System with Updated Trim Value Data Applied to Nonlinear Simulation at Baseline Condition #2, Negative Bias Case

Simulation Scenario #	Isolated Minimum Positive Bias in % of Nominal Trim Value (Euclidian distance of health parameter estimation errors in parentheses)										
	XN2	XN25	T27D	T56	PS15	P27	PS3	PS56	WF36	A8	A16
1	-3.3 (0.11)	-0.8 (0.01)	-1.3 (0.01)	-2.4 (0.01)	-13.8 (0.07)	-3.3 (0.01)	-1.3 (0.05)	-4.3 (0.05)	-2.6 (0.01)	-5.1 (0.06)	-27.6 (0.02)
2	-3.3 (0.47)	-1.1 (0.20)	-1.3 (0.20)	-2.4 (0.17)	-12.3 (0.22)	-3.8 (0.23)	-1.4 (0.20)	-4.4 (0.21)	-2.7 (0.20)	-6.5 (0.18)	-32.1 (0.21)
3	-3.5 (0.46)	-1.0 (0.58)	-1.2 (0.59)	-2.5 (0.58)	-10.3 (0.60)	-3.5 (0.56)	-1.2 (0.59)	-4.0 (0.59)	-3.0 (0.59)	-6.2 (0.56)	-34.1 (0.57)
4	-3.4 (0.29)	-1.2 (0.44)	-1.2 (0.50)	-2.7 (0.51)	-9.3 (0.48)	-3.5 (0.37)	-1.4 (0.46)	-4.3 (0.49)	-3.0 (0.49)	-6.8 (0.42)	-33.3 (0.46)
5	-2.8 (0.92)	-1.0 (1.07)	-1.3 (1.08)	-2.5 (1.07)	-10.2 (1.07)	-3.4 (0.99)	-1.3 (1.08)	-3.4 (1.07)	-2.7 (1.09)	-5.6 (1.09)	-31.5 (1.06)
6	-2.7 (0.47)	-1.0 (0.98)	-1.2 (1.02)	-2.5 (0.99)	-10.0 (0.98)	-3.4 (0.87)	-1.3 (1.00)	-3.4 (0.98)	-2.8 (1.00)	-5.5 (0.98)	-30.5 (1.00)
7	-3.4 (1.41)	-1.1 (1.58)	-1.3 (1.57)	-2.7 (1.56)	-11.6 (1.56)	-3.0 (1.38)	-1.5 (1.58)	-4.1 (1.56)	-3.0 (1.58)	-5.9 (1.56)	-32.5 (1.53)
8	-3.4 (0.84)	-1.0 (1.53)	-1.2 (1.54)	-2.8 (1.50)	-11.4 (1.49)	-3.2 (1.31)	-1.5 (1.51)	-4.2 (1.50)	-3.1 (1.51)	-5.9 (1.49)	-32.9 (1.50)

b. Baseline Condition #3

Tables 10 and 11 show the performance evaluation results when the FDI system is applied to the nonlinear simulation at baseline condition #3. Table 10 shows the positive bias case while Table 11 shows the negative bias case. Again, the trim value data has been updated so that the initial steady-state mismatch is eliminated. No false alarms were generated on any simulation scenario with sensor/actuator bias (88+88 cases) or without sensor/actuator bias (8 scenarios).

As seen in the previous case of baseline condition #2, a similar trend can be observed; the sensor/actuator FDI performance can be recovered by updating the trim value data. The health parameter estimation accuracy, however, worsens compared to the previous case. As the baseline degradation worsens, the mismatch in the dynamics between the FDI system and the nonlinear simulation increases and the "smearing" effect becomes more prominent. This example indicates that large health parameter estimation errors do not necessarily result in large sensor estimation errors. Therefore, determining the confidence in estimated health parameters, which is currently based on sensor estimation errors, is always a challenging issue in the health estimation problem. With the current FDI design, component faults can be inferred from changes in the estimated health parameters; however, the corresponding damage level cannot be estimated accurately.

Table 10. Performance of the FDI System with Updated Trim Value Data Applied to Nonlinear Simulation at Baseline Condition #3, Positive Bias Case

Simulation Scenario #	Isolated Minimum Positive Bias in % of Nominal Trim Value (Euclidian distance of health parameter estimation errors in parentheses)										
	XN2	XN25	T27D	T56	PS15	P27	PS3	PS56	WF36	A8	A16
1	3.5 (0.14)	0.8 (0.01)	1.4 (0.03)	2.8 (0.03)	11.6 (0.07)	3.2 (0.01)	1.4 (0.01)	4.8 (0.05)	2.6 (0.01)	5.5 (0.04)	25.1 (0.02)
2	3.5 (0.83)	1.1 (0.41)	1.4 (0.43)	2.5 (0.34)	13.2 (0.38)	3.7 (0.37)	1.5 (0.40)	4.2 (0.41)	2.9 (0.45)	6.7 (0.41)	29.2 (0.41)
3	3.1 (0.55)	0.9 (0.68)	1.2 (0.68)	2.2 (0.68)	11.3 (0.70)	3.3 (0.62)	1.5 (0.72)	4.2 (0.70)	3.0 (0.68)	5.8 (0.69)	32.0 (0.67)
4	3.5 (0.41)	1.0 (0.60)	1.4 (0.64)	2.1 (0.61)	11.4 (0.60)	3.4 (0.34)	1.5 (0.63)	4.2 (0.63)	3.1 (0.61)	5.2 (0.59)	31.4 (0.59)
5	3.0 (1.29)	0.9 (1.30)	1.1 (1.30)	2.4 (1.28)	9.9 (1.26)	3.6 (1.19)	1.4 (1.33)	3.8 (1.30)	2.6 (1.34)	4.8 (1.32)	27.0 (1.28)
6	3.1 (0.44)	1.0 (1.19)	1.1 (1.23)	2.2 (1.19)	9.9 (1.18)	3.7 (0.95)	1.4 (1.22)	3.9 (1.20)	2.9 (1.20)	4.8 (1.19)	26.6 (1.21)
7	3.6 (2.11)	1.0 (1.89)	1.3 (1.88)	2.8 (1.85)	11.3 (1.87)	3.2 (1.74)	1.4 (1.91)	4.6 (1.88)	3.1 (1.92)	5.9 (1.94)	34.3 (1.84)
8	3.6 (1.14)	1.1 (1.79)	1.4 (1.82)	2.6 (1.78)	11.5 (1.79)	3.1 (1.54)	1.4 (1.81)	4.3 (1.76)	3.0 (1.81)	6.2 (1.77)	33.8 (1.79)

Table 11. Performance of the FDI System with Updated Trim Value Data Applied to Nonlinear Simulation at Baseline Condition #3, Negative Bias Case

Simulation Scenario #	Isolated Minimum Positive Bias in % of Nominal Trim Value (Euclidian distance of health parameter estimation errors in parentheses)										
	XN2	XN25	T27D	T56	PS15	P27	PS3	PS56	WF36	A8	A16
1	-3.5 (0.14)	-0.8 (0.01)	-1.3 (0.01)	-2.4 (0.01)	-13.6 (0.07)	-3.3 (0.01)	-1.3 (0.04)	-4.3 (0.05)	-2.6 (0.01)	-5.1 (0.07)	-27.5 (0.03)
2	-3.4 (0.84)	-1.1 (0.41)	-1.3 (0.41)	-2.7 (0.32)	-11.9 (0.38)	-3.6 (0.35)	-1.4 (0.40)	-4.6 (0.41)	-2.9 (0.40)	-5.9 (0.41)	-32.8 (0.42)
3	-3.3 (0.61)	-1.0 (0.67)	-1.3 (0.69)	-2.5 (0.70)	-11.9 (0.70)	-3.5 (0.61)	-1.3 (0.69)	-3.8 (0.70)	-2.9 (0.72)	-6.6 (0.68)	-27.6 (0.67)
4	-3.4 (0.43)	-1.0 (0.61)	-1.2 (0.66)	-2.7 (0.63)	-10.6 (0.60)	-3.5 (0.36)	-1.3 (0.62)	-4.1 (0.63)	-3.1 (0.63)	-6.5 (0.55)	-30.9 (0.61)
5	-2.8 (1.27)	-1.0 (1.29)	-1.3 (1.30)	-2.2 (1.28)	-10.6 (1.26)	-3.7 (1.20)	-1.4 (1.33)	-3.4 (1.30)	-2.7 (1.33)	-5.8 (1.34)	-26.9 (1.28)
6	-2.9 (0.49)	-0.9 (1.21)	-1.2 (1.25)	-2.5 (1.21)	-10.1 (1.18)	-3.6 (0.95)	-1.5 (1.21)	-3.5 (1.20)	-2.8 (1.22)	-6.0 (1.18)	-26.8 (1.21)
7	-3.4 (2.11)	-1.2 (1.89)	-1.4 (1.88)	-2.6 (1.85)	-12.2 (1.87)	-3.0 (1.76)	-1.4 (1.91)	-4.1 (1.88)	-2.9 (1.93)	-6.1 (1.93)	-32.4 (1.84)
8	-3.3 (1.14)	-1.0 (1.77)	-1.3 (1.83)	-2.8 (1.77)	-12.0 (1.79)	-3.1 (1.55)	-1.4 (1.81)	-4.3 (1.77)	-3.0 (1.80)	-6.0 (1.80)	-32.8 (1.79)

3) FDI Performance Recovery Through Updating the Bank of Kalman Filters

In this section, the bank of Kalman filters is updated to account for baseline degradation. The updated FDI system is then applied to the nonlinear simulation at baseline conditions #2 and #3. Since the bank of Kalman filters is designed at new trim conditions, the trim value data is also updated. Therefore, the initial steady-state values and the dynamics of the FDI system match with those of the nonlinear simulation.

a. Baseline Condition #2

Tables 12 and 13 show the performance evaluation results when the FDI system is applied to the nonlinear simulation at baseline condition #2. Table 12 shows the positive bias case while Table 13 shows the negative bias case. No false alarms were generated on any simulation scenario with sensor/actuator bias (88+88 cases) or without sensor/actuator bias (8 scenarios).

From the tables, it can be observed that the primary benefit of updating the bank of Kalman filters based on the baseline condition is the improved accuracy of the health parameter estimation. When the trim value data alone was updated, the health parameter estimation error exceeded 0.5% in 43 of 88 cases as seen in Tables 8 and 9. When the bank of Kalman filters is updated, only one case (Scenario 8 for the XN2 bias) violated the 0.5% estimation error bound.

The benefit of isolating bias at the smaller magnitude level can be observed most prominently in the XN2 sensor. Some benefits are also seen in XN25, T27D, P27, PS3, PS56, and A8. However, the magnitudes of the isolated bias in T56, PS15, and A16 are much higher in this case than the previous case where the trim value data alone was updated.

Table 12. Performance of the FDI System with Updated Bank of Kalman Filters Applied to Nonlinear Simulation at Baseline Condition #2, Positive Bias Case

Simulation Scenario #	Isolated Minimum Positive Bias in % of Nominal Trim Value (Euclidian distance of health parameter estimation errors in parentheses)										
	XN2	XN25	T27D	T56	PS15	P27	PS3	PS56	WF36	A8	A16
1	2.6 (0.10)	1.1 (0.03)	1.4 (0.01)	2.6 (0.04)	13.7 (0.07)	3.6 (0.02)	1.3 (0.01)	4.9 (0.05)	2.9 (0.01)	6.2 (0.01)	42.1 (0.04)
2	2.4 (0.48)	1.0 (0.19)	1.2 (0.11)	3.2 (0.16)	13.7 (0.30)	2.8 (0.12)	1.2 (0.16)	4.9 (0.16)	3.1 (0.15)	6.2 (0.34)	41.6 (0.14)
3	2.5 (0.11)	1.0 (0.13)	1.3 (0.13)	3.1 (0.08)	12.0 (0.11)	3.2 (0.11)	1.1 (0.13)	3.8 (0.13)	3.1 (0.15)	5.2 (0.15)	42.4 (0.12)
4	2.5 (0.53)	1.0 (0.10)	1.2 (0.09)	3.1 (0.10)	11.2 (0.21)	3.2 (0.15)	1.0 (0.12)	3.7 (0.20)	3.3 (0.10)	4.5 (0.44)	44.8 (0.05)
5	1.9 (0.26)	0.9 (0.14)	1.1 (0.10)	2.4 (0.06)	11.7 (0.11)	3.6 (0.09)	1.2 (0.12)	3.5 (0.15)	3.1 (0.11)	5.9 (0.24)	34.3 (0.10)
6	1.9 (0.74)	0.8 (0.08)	1.1 (0.04)	2.5 (0.10)	11.7 (0.21)	3.5 (0.22)	1.2 (0.07)	3.6 (0.14)	3.1 (0.07)	5.6 (0.40)	34.3 (0.12)
7	2.1 (0.49)	0.9 (0.20)	1.1 (0.19)	2.6 (0.18)	12.0 (0.24)	3.0 (0.16)	1.3 (0.17)	3.9 (0.20)	3.1 (0.16)	5.9 (0.38)	40.9 (0.20)
8	2.1 (0.86)	0.8 (0.17)	1.1 (0.14)	2.6 (0.22)	11.9 (0.36)	2.9 (0.36)	1.3 (0.16)	3.9 (0.10)	3.1 (0.15)	5.8 (0.27)	41.1 (0.24)

Table 13. Performance of the FDI System with Updated Bank of Kalman Filters Applied to Nonlinear Simulation at Baseline Condition #2, Negative Bias Case

Simulation Scenario #	Isolated Minimum Positive Bias in % of Nominal Trim Value (Euclidian distance of health parameter estimation errors in parentheses)										
	XN2	XN25	T27D	T56	PS15	P27	PS3	PS56	WF36	A8	A16
1	-2.7 (0.07)	-1.2 (0.03)	-1.4 (0.01)	-2.5 (0.03)	-15.4 (0.07)	-3.6 (0.01)	-1.3 (0.01)	-4.4 (0.05)	-2.6 (0.02)	-7.7 (0.05)	-44.5 (0.04)
2	-2.4 (0.48)	-1.1 (0.19)	-1.3 (0.12)	-2.9 (0.17)	-14.7 (0.30)	-3.1 (0.12)	-1.3 (0.14)	-4.6 (0.16)	-3.1 (0.16)	-6.3 (0.38)	-38.6 (0.14)
3	-2.6 (0.11)	-1.2 (0.13)	-1.2 (0.12)	-2.4 (0.11)	-11.1 (0.11)	-3.2 (0.11)	-1.6 (0.14)	-3.8 (0.13)	-2.5 (0.14)	-7.1 (0.19)	-41.2 (0.14)
4	-2.5 (0.53)	-1.2 (0.10)	-1.2 (0.11)	-2.2 (0.12)	-10.7 (0.21)	-3.3 (0.15)	-1.6 (0.09)	-3.3 (0.20)	-2.3 (0.12)	-7.8 (0.47)	-40.9 (0.04)
5	-2.1 (0.26)	-0.8 (0.13)	-1.1 (0.12)	-2.3 (0.10)	-11.2 (0.11)	-3.2 (0.09)	-1.3 (0.11)	-3.4 (0.15)	-2.6 (0.14)	-7.3 (0.22)	-38.1 (0.13)
6	-2.2 (0.74)	-0.8 (0.07)	-1.2 (0.04)	-2.3 (0.08)	-11.3 (0.21)	-3.3 (0.21)	-1.3 (0.07)	-3.3 (0.14)	-2.6 (0.08)	-7.5 (0.38)	-38.1 (0.08)
7	-2.2 (0.49)	-0.9 (0.20)	-1.2 (0.19)	-2.5 (0.18)	-12.4 (0.24)	-3.2 (0.15)	-1.3 (0.17)	-3.4 (0.20)	-2.8 (0.16)	-6.6 (0.38)	-37.7 (0.20)
8	-2.2 (0.86)	-1.0 (0.17)	-1.2 (0.14)	-2.5 (0.22)	-12.4 (0.36)	-3.2 (0.36)	-1.3 (0.16)	-3.3 (0.10)	-2.7 (0.14)	-6.6 (0.27)	-37.4 (0.24)

b. Baseline Condition #3

Tables 14 and 15 show the performance evaluation results when the FDI system is applied to the nonlinear simulation at baseline condition #3. Table 14 shows the positive bias case while Table 15 shows the negative bias case. No false alarms were generated on any simulation scenario with sensor/actuator bias (88+88 cases) or without sensor/actuator bias (8 scenarios).

Unlike the previous case shown in Tables 12 and 13 (baseline condition #2), improved health parameter estimation accuracy is not seen in this case. It is suspected that the reason for not obtaining better estimation accuracy is due to linearization error playing a significant role in this example. In all of the eight simulation scenarios, the steady-state responses of the sensor measurements were compared between the linear engine model and the nonlinear simulation. For baseline condition #3, a large steady-state response (i.e., steady-state gain) error was found in the XN2 sensor measurement. As the health parameter perturbations increased to 1%, 2%, and 3%, the XN2 error worsened to 0.1%, 0.22%, and 0.35% of the nominal trim value, respectively. These errors are quite large relative to the standard deviation of noise on this measurement (Table 2). The XN2 error due to linearization appears like a bias and consequently corrupts the performance of all FDI filters, except for filter #1. Since FDI filter #1 does not use the measurement XN2, it performs well in the presence of this linearization error as seen in Tables 14 and 15. (For baseline degradation condition #1, the worst steady-state response error was 0.3% in PS3 for scenario 7. For baseline degradation condition #2, the worst steady-state response error was 0.08% in T56 for scenario 2.)

The benefit of isolating bias at the smaller magnitude level can be observed most prominently in the XN2 sensor. Some benefit is also seen in P27. However, the magnitudes of the isolated bias in T56, PS15, PS56, WF36, A8, and A16 are much higher in this case than the previous case where the trim value data alone was updated.

Table 14. Performance of the FDI System with Updated Bank of Kalman Filters Applied to Nonlinear Simulation at Baseline Condition #3, Positive Bias Case

Simulation Scenario #	Isolated Minimum Positive Bias in % of Nominal Trim Value (Euclidian distance of health parameter estimation errors in parentheses)										
	XN2	XN25	T27D	T56	PS15	P27	PS3	PS56	WF36	A8	A16
1	2.1 (0.22)	1.1 (0.04)	1.4 (0.13)	3.6 (0.07)	14.2 (0.04)	3.1 (0.04)	1.6 (0.06)	5.5 (0.06)	3.3 (0.06)	7.6 (0.05)	43.5 (0.02)
2	2.0 (0.31)	1.0 (0.26)	1.3 (0.10)	3.5 (0.16)	13.8 (0.32)	3.2 (0.15)	1.5 (0.14)	5.6 (0.19)	3.4 (0.13)	7.6 (0.47)	43.8 (0.18)
3	1.8 (0.07)	1.0 (0.64)	1.3 (0.67)	3.6 (0.59)	16.7 (0.52)	3.3 (0.36)	1.6 (0.51)	5.2 (0.52)	3.2 (0.53)	7.2 (0.52)	48.8 (0.54)
4	2.0 (0.39)	0.9 (0.32)	1.3 (0.58)	3.7 (0.46)	15.7 (0.57)	3.3 (0.30)	1.5 (0.40)	5.4 (0.40)	3.2 (0.40)	6.7 (0.60)	48.9 (0.51)
5	1.8 (0.17)	1.0 (1.31)	1.3 (1.46)	3.3 (1.28)	11.2 (1.14)	3.2 (0.79)	1.4 (1.11)	4.5 (1.11)	3.3 (1.10)	6.5 (1.12)	44.7 (1.17)
6	1.7 (0.47)	1.0 (1.01)	1.2 (1.33)	3.4 (1.17)	11.3 (1.11)	3.2 (0.71)	1.3 (0.95)	4.7 (0.93)	3.4 (0.95)	6.0 (1.01)	44.4 (1.08)
7	1.7 (0.30)	1.2 (2.14)	1.3 (2.40)	3.7 (2.11)	15.0 (1.94)	2.9 (1.30)	1.5 (1.84)	4.3 (1.83)	4.0 (1.82)	5.4 (1.87)	35.2 (1.93)
8	1.7 (0.57)	1.2 (1.92)	1.2 (2.21)	3.7 (1.94)	14.9 (1.82)	2.9 (1.23)	1.5 (1.67)	4.4 (1.64)	4.0 (1.65)	5.3 (1.67)	35.6 (1.80)

Table 15. Performance of the FDI System with Updated Bank of Kalman Filters Applied to Nonlinear Simulation at Baseline Condition #3, Negative Bias Case

Simulation Scenario #	Isolated Minimum Positive Bias in % of Nominal Trim Value (Euclidian distance of health parameter estimation errors in parentheses)										
	XN2	XN25	T27D	T56	PS15	P27	PS3	PS56	WF36	A8	A16
1	-2.0 (0.22)	-1.0 (0.04)	-1.5 (0.12)	-3.7 (0.05)	-16.2 (0.04)	-3.1 (0.03)	-1.5 (0.06)	-4.6 (0.06)	-3.6 (0.03)	-8.0 (0.02)	-38.6 (0.01)
2	-2.2 (0.32)	-1.1 (0.21)	-1.5 (0.10)	-3.4 (0.16)	-15.8 (0.32)	-3.4 (0.15)	-1.6 (0.15)	-4.5 (0.19)	-3.4 (0.12)	-8.4 (0.46)	-39.9 (0.17)
3	-1.8 (0.08)	-0.9 (0.64)	-1.3 (0.66)	-3.1 (0.59)	-15.4 (0.52)	-3.2 (0.37)	-1.3 (0.52)	-5.0 (0.52)	-3.5 (0.52)	-8.6 (0.52)	-43.9 (0.50)
4	-1.8 (0.39)	-1.0 (0.31)	-1.2 (0.58)	-3.1 (0.47)	-15.4 (0.57)	-3.2 (0.30)	-1.3 (0.38)	-4.7 (0.40)	-3.2 (0.39)	-8.8 (0.57)	-43.9 (0.50)
5	-1.8 (0.19)	-0.9 (1.26)	-1.2 (1.47)	-2.8 (1.24)	-12.7 (1.15)	-3.2 (0.79)	-1.2 (1.14)	-4.4 (1.10)	-3.1 (1.09)	-6.8 (1.12)	-39.9 (1.16)
6	-0.17 (0.52)	-0.9 (0.96)	-1.4 (1.34)	-2.7 (1.09)	-12.9 (1.11)	-3.2 (0.71)	-1.2 (0.97)	-4.0 (0.93)	-3.0 (0.94)	-6.6 (1.02)	-39.7 (1.09)
7	-2.0 (0.30)	-0.9 (2.11)	-1.5 (2.40)	-2.6 (2.06)	-15.2 (1.94)	-3.1 (1.32)	-1.5 (1.86)	-4.3 (1.84)	-2.8 (1.80)	-7.1 (1.91)	-35.1 (1.95)
8	-2.1 (0.57)	-0.9 (1.86)	-1.5 (2.21)	-2.6 (1.89)	-15.3 (1.82)	-3.1 (1.24)	-1.5 (1.69)	-4.2 (1.65)	-2.8 (1.62)	-7.3 (1.71)	-34.6 (1.81)

8.0 Concluding Remarks

An FDI system which utilizes a bank of Kalman filters with an augmented state vector was developed for aircraft engine sensor/actuator FDI in conjunction with the detection of component faults. Each Kalman filter was designed to detect a specific sensor or actuator fault while estimating the selected four health parameters which could degrade abruptly. Based on the fault isolation logic, one filter in the bank was isolated from the rest, and consequently the isolated filter itself indicated which sensor or actuator had failed. Moreover, the FDI filter using the "correct" fault hypothesis detected component faults by estimating the four health parameters from the fault-free sensor measurements.

The performance of the FDI system was evaluated against the nonlinear engine simulation at cruise operating conditions. The performance was evaluated based on the minimum magnitude of the isolated sensor/actuator bias and the accuracy of the health parameter estimation. Eight simulation scenarios, where the selected four health parameters and the control commands were perturbed, were investigated. The perturbations in the four health parameters represented abrupt component degradation due to a FOD event, while the control command perturbations disturbed engine operating condition.

Furthermore, the "baseline degradation" was used in order to investigate the benefit of incorporating information regarding the engine's aging condition in the FDI system. It is well known that the physical engine components deteriorate gradually due to wear and tear on blades and the casing as an engine operates over time. Such an aging phenomenon was referred to as baseline degradation and represented by a set of deviations in all 10 health parameters from the healthy baseline condition. When the FDI system designed at the healthy baseline condition was applied to the healthy engine (nonlinear simulation at baseline condition #1), the FDI system performed well in most of the simulation scenarios. When the same FDI system was applied to the aging engine (nonlinear simulation at baseline conditions #2 and #3), the deviations in all 10 health parameters were "smeared" to the four health parameters being estimated, resulting in unacceptable health parameter estimation accuracy. Moreover, multiple FDI filters generated false alarms. If an FDI system which does not account for baseline degradation is applied to a physical aged engine, the same results can be expected. The performance loss of the FDI system due to the aging effects was partially recovered by updating either 1) the trim value data or 2) the bank of Kalman filters.

When the trim value data was updated based on the baseline degradation, the mismatch in the steady-state condition values at the initial trim point between the "nominal" FDI system and the "aged" nonlinear engine simulation was eliminated, and consequently the ability of isolating the sensor and actuator fault was retained for both aging conditions (baseline degradations #2 and #3). However, the accuracy of estimating health parameters was not as good as the nominal baseline case. Although the initial steady-state condition values were made to match, the mismatch in the dynamics caused errors in the steady-state response (i.e., steady-state gain) after health parameter and control command perturbations, resulting in the loss of estimation accuracy.

In order to regain the estimation accuracy, the bank of Kalman filters was updated based on the baseline degradation. Since both the initial steady-state condition values and the dynamics matched between the FDI system and the nonlinear engine simulation at the degraded baseline condition, the accuracy of the health parameter estimation was significantly improved for baseline condition #2. Also, a benefit of isolating bias at a lower magnitude was observed in some of the sensors.

For baseline condition #3, the aforementioned benefits of updating the bank of Kalman filters were not observed. The accuracy of the health parameter estimation was low, and the isolated bias magnitudes were much higher than the case where the trim value data alone was updated. It was found that, when multiple health parameters were perturbed, a large difference in the steady-state response of the XN2

measurement existed between the linear engine model and the nonlinear engine simulation, even though the baseline degradation matched. This steady-state response error in XN2 was suspected as the cause of the unsatisfactory results. It is not known whether this steady-state error is due to the linearization process or the nonlinear effects at this baseline condition. However, this example reveals the significance of the linear model accuracy in order to accurately estimate the health parameters. In this paper, it is assumed that the baseline degradation is tracked by the steady-state condition monitoring system, and the linear models are generated at new baseline conditions. For this approach to be practical, further research is needed on how the linear models are to be generated and validated.

Significant robustness in terms of detecting and isolating sensor and actuator faults was observed by updating the trim value data or the bank of Kalman filters. For a total of 920 simulation cases investigated in this paper, the FDI system did not generate a false alarm. It is considered that the augmented state vector, which was incorporated into the Kalman filter design for health parameter estimation, played a significant role. The initial objective of estimating a selected set of health parameters was to avoid a scenario where abrupt component degradation is incorrectly identified as a sensor or actuator fault by the FDI system. This objective was satisfied in all simulation cases. When both the initial steady-state and the dynamics of the FDI system matched with that of the nonlinear engine simulation, the Kalman filters accurately estimated the selected four health parameters. When the dynamics of the FDI system did not match well with that of the nonlinear engine simulation, the Kalman filters "tuned" these selected health parameters so that the measurement estimates will match with the outputs of the nonlinear simulation. Because of this "tuning" effect, low sensor estimation errors were retained, and as a result, no false alarm was generated.

For further research, it is interesting to use a subset of the 10 health parameters as a tuner for improvement of the FDI performance. The idea of parameter tuning has been investigated in the adaptive control area.[27,28] In this paper, abrupt component degradation due to a FOD event was modeled as step changes in the health parameters of a fan and a booster. During a flight, some other component faults can happen such as domestic object damage (DOD) due to failed HPC or HPT blades. If such faults happened, it is not known how the current FDI system would react. The best approach to capture the all component faults is to estimate all 10 health parameters. However, the number and the location of the available sensors restrict the estimation accuracy. If a subset of the health parameters is used as a tuner, it is expected that the sensor and actuator FDI performance would be retained even in the event of FOD, DOD, or other component faults. A drawback of using a subset of health parameters as a tuner is that those selected parameters no longer represent the actual health parameters, thus the purpose of estimating the component damage is compromised.

It is also interesting to assess the FDI performance using modified fault indicator signals (i.e., WSSR). As previously discussed, some pairs of FDI filters were difficult to isolate from each other; however, a "wrong" filter usually generated health parameter estimates well beyond the expected linear range. Incorporating such information in the fault indicator signal may help in isolating between a troublesome pair of FDI filters at a much smaller bias level. In future work, the above issues will be considered in addition to extending the FDI capability over a wider flight region.

9.0 References

[1] Frank, P. M., "Fault Diagnosis in Dynamic Systems Using Analytical and Knowledge-based Redundancy – A Survey and Some New Results," *Automatica*, Vol. 26, No. 3, pp. 459-474, 1990.

[2] Patton, R. J., and Chen, J., "Robust Fault Detection of Jet Engine Sensor Systems Using Eigenstructure Assignment," Journal of Guidance, Control, and Dynamics, Vol. 15, No. 6, Nov-Dec 1992.

[3] Merrington, G., Kwon, O.-K., Goodwin, G., and Carlsson, B., "Fault Detection and Diagnosis in Gas Turbines," Journal of Engineering for Gas Turbines and Power, pp. 276-282, Vol. 113, April 1991.

[4] Khargonekar, P. P., and Ting T. L., "Fault Detection in the Presence of Modeling Uncertainty," IEEE Proceedings of the 32nd Conference on Decision and Control, pp. 1716-1721, December 1993.

[5] Patton, R. J., Zhang, H. Y., and Chen, J., "Modeling of Uncertainties for Robust Fault Diagnosis," IEEE Proceedings of the 31st Conference on Decision and Control, pp. 921-926, December 1992.

[6] Patton, R. J., Chen, J., and Zhang, H. Y., "Modeling Methods for Improving Robustness in Fault Diagnosis of Jet Engine System," IEEE Proceedings of the 31st Conference on Decision and Control, pp. 2330-2335, December 1992.

[7] Volponi, A. J, DePold, H., Ganguli, R., and Daguang, C., 2000, "The Use of Kalman Filter and Neural Network Methodologies in Gas Turbine Performance Diagnostics: A Comparative Study," ASME Paper 2000-GT-547, Proceedings of ASME TURBOEXPO 2000, Munich, Germany.

[8] Merrill, W. C., DeLaat, J. C., and Bruton, W. M., "Advanced Detection, Isolation, and Accommodation of Sensor Failures – Real-Time Evaluation," Journal of Guidance, Control, and Dynamics, pp. 517-526, Vol. 11, No. 6, Nov-Dec 1988.

[9] Duyar, A., Eldem, V., Merrill, W., and Guo, T.-H., "Fault Detection and Diagnosis in Propulsion Systems: A Fault Parameter Estimation Approach," Journal of Guidance, Control, and Dynamics, pp. 104-108, Vo. 17, No. 1, Jan-Feb 1994.

[10] Menke, T. E., and Maybeck, P. S., "Sensor/Actuator Failure Detection in the Vista F-16 by Multiple Model Adaptive Estimation," IEEE Transactions on Aerospace and Electronic Systems, pp. 1218-1229, Vol. 31, No. 4, October 1995.

[11] Hajiyev, C., and Caliskan, F., "Sensor/Actuator Fault Diagnosis Based on Statistical Analysis of Innovation Sequence and Robust Kalman Filtering," Aerospace Science & Technology, 4, pp. 415-422, September 2000.

[12] Stamatis, A., Mathioudakis, K., Berios, G., and Papailiou, K., "Jet Engine Fault Detection with Differential Gas Path Analysis at Discrete Operating Points," ISABE 89-7133.

[13] Volponi, A. J., "Sensor Error Compensation in Engine Performance Diagnostics," ASME Paper 94-GT-58, International Gas Turbine and Aeroengine Congress and Exposition, The Hague, Netherlands, 1994.

[14] DePold, H. R., and Gass, F. D., "The Application of Expert Systems and Neural Networks to Gas Turbine Prognostics and Diagnostics," Journal of Engineering for Gas Turbines and Power, pp. 607-612, Vol. 121, October 1999.

[15] Kobayashi, T., and Simon, D. L., "A Hybrid Neural Network-Genetic Algorithm Technique for Aircraft Engine Performance Diagnostics," Paper AIAA-2001-3763, AIAA 37th Joint Propulsion Conference, Salt Lake City, UT, 2001.

[16] Adibhatla, S., and Lewis, T. J., "Model-Based Intelligent Digital Engine Control (MoBIDEC)," Paper AIAA-97-3192, AIAA 33rd Joint Propulsion Conference, Seattle, WA, 1997.

[17] Lakshminarasimha, A. N., Boyce, M. P., and Meher-Homji, C. B., "Modeling and Analysis of Gas Turbine Performance Deterioration," Journal of Engineering for Gas Turbines and Power, pp46-52, Vol. 116, January 1994.

[18] Diakunchak, I. S., "Performance Detrioration in Industrial Gas Turbines," Journal of Engineering for Gas Turbines and Power, pp. 161-168, Vol. 114, April 1992.

[19] Tabakoff, W., Lakshminarasimha, A. N., and Pasin, M., "Simulation of Compressor Performance Deterioration Due to Erosion," Journal of Turbomachinery, pp. 78-83, Vol. 112, January 1990.

[20] Batcho, P. F., Moller, J. C., Padova, C., and Dunn, M. G., "Interpretation of Gas Turbine Response Due to Dust Ingestion," Journal of Engineering for Gas Turbines and Power, pp. 344-352, Vol. 109, July 1987.

[21] Richardson, J. H., Sallee, G. P., and Smakula, F. K., "Causes of High Pressure Compressor Detrioration in Service," Paper AIAA-79-1234, AIAA 15th Joint Propulsion Conference, Las Vegas, NV, 1979.

[22] Lambert, H. H., "A Simulation Study of Turbofan Engine Deterioration Estimation Using Kalman Filtering Techniques," NASA TM-104233, 1991.

[23] España, M. D., and Gilyard, G. B., "On the Estimation Algorithm Used in Adaptive Performance Optimization of Turbofan Engines," NASA TM-4551, 1993.

[24] Lu, P.-J., Zhang, M.-C., Hsu, T.-C., and Zhang, J., "An Evaluation of Engine Faults Diagnostics Using Artificial Neural Networks," Journal of Engineering for Gas Turbines and Power, pp. 340-346, Vol. 123, April 2001.

[25] Pinelli, M., and Spina, P. R., "Gas Turbine Field Performance Determination: Sources of Uncertainties," Journal of Engineering for Gas Turbines and Power, pp. 155-160, Vol. 124, January 2002.

[26] Kerr, L. J., Nemec, T. S., and Gallops, G. W., "Real-Time Estimation of Gas Turbine Engine Damage Using a Control Based Kalman Filter Algorithm," ASME Paper 91-GT-216, International Gas Turbine and Aeroengine Congress and Exposition, Orlando, FL, 1991.

[27] Luppold, R. H., Roman, J. R., Gallops, G. W., and Kerr, L. J., "Estimating In-Flight Engine Performance Variations Using Kalman Filter Concepts," Paper AIAA-89-2584, AIAA 25th Joint Propulsion Conference, Monterey, CA, 1989.

[28] Adibhatla, S., and Gastineau, Z., "Tracking Filter Selection and Control Mode Selection for Model Based Control," Paper AIAA-94-3204, AIAA 30th Joint Propulsion Conference, Indianapolis, IN, 1994.

Appendix

The actuator bias can be injected either in the actuator inputs or actuator outputs as shown in Figures 10 and 11. Although Equation (9) incorporates the actuator bias vector in the actuator inputs, it can be easily modified such that the bias vector is incorporated in the actuator outputs.

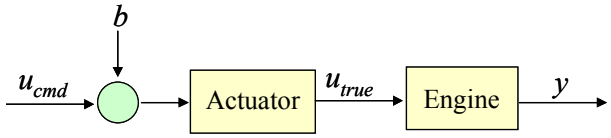

Figure 10. Actuator Bias Added to the Actuator Input Vector

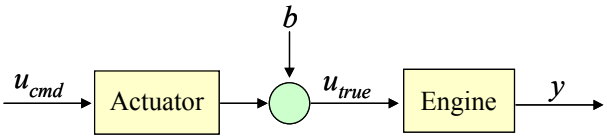

Figure 11. Actuator Bias Added to the Actuator Output Vector

Let the state-space model of the engine be given by:

$$\begin{aligned} \dot{x}_{eng} &= A_{eng} x_{eng} + B_{eng} u_{true} \\ y &= C_{eng} x_{eng} + D_{eng} u_{true} \end{aligned} \tag{14}$$

Let the state-space model of the actuator be given by:

$$\begin{aligned} \dot{x}_{act} &= A_{act} x_{act} + B_{act} u_{cmd} \\ u_{true} &= C_{act} x_{act} + D_{act} u_{cmd} \end{aligned} \tag{15}$$

When the engine and actuator state-space models are combined, the combined state-space model is given as (assume that "0" and "I" in the following equations are the matrices with appropriate dimensions):

$$\dot{x} = Ax + B_1 u_{cmd} + B_2 b$$
$$y = Cx + D_1 u_{cmd} + D_2 b \tag{16}$$

where

$$x = \begin{bmatrix} x_{eng} \\ x_{act} \end{bmatrix}, \quad A = \begin{bmatrix} A_{eng} & B_{eng} C_{act} \\ 0 & A_{act} \end{bmatrix}, \quad C = \begin{bmatrix} C_{eng} & D_{eng} C_{act} \end{bmatrix}$$

If the bias vector is added to the actuator inputs as shown in Figure 10:

$$B_1 = B_2 = \begin{bmatrix} B_{eng} D_{act} \\ B_{act} \end{bmatrix}$$
$$D_1 = D_2 = D_{eng} D_{act} \tag{17}$$

If the bias vector is added to the actuator outputs as shown in Figure 11:

$$B_1 = \begin{bmatrix} B_{eng} D_{act} \\ B_{act} \end{bmatrix}, \quad B_2 = \begin{bmatrix} B_{eng} \\ 0 \end{bmatrix}$$
$$D_1 = D_{eng} D_{act}, \quad D_2 = D_{eng} \tag{18}$$

If the engine dynamics are ignored as the example given in this paper (See Section 3.0), the actuator state-space model (Equation 15) reduces to:

$$A_{act} = 0, \quad B_{act} = 0, \quad C_{act} = 0, \quad D_{act} = \mathrm{I}$$

Therefore, Equations (17) and (18) are equivalent.

REPORT DOCUMENTATION PAGE

Form Approved
OMB No. 0704-0188

1. AGENCY USE ONLY (*Leave blank*)	2. REPORT DATE	3. REPORT TYPE AND DATES COVERED
	March 2003	Final Contractor Report

4. TITLE AND SUBTITLE

Aircraft Engine Sensor/Actuator/Component Fault Diagnosis Using a Bank of Kalman Filters

5. FUNDING NUMBERS

WBS–22–728–30–05
NAS3–00145

6. AUTHOR(S)

Takahisa Kobayashi

7. PERFORMING ORGANIZATION NAME(S) AND ADDRESS(ES)

QSS Group, Inc.
21000 Brookpark Road
Cleveland, Ohio 44135

8. PERFORMING ORGANIZATION REPORT NUMBER

E–13862

9. SPONSORING/MONITORING AGENCY NAME(S) AND ADDRESS(ES)

National Aeronautics and Space Administration
Washington, DC 20546–0001

10. SPONSORING/MONITORING AGENCY REPORT NUMBER

NASA CR—2003-212298

11. SUPPLEMENTARY NOTES

Project Manager, Donald L. Simon, Instrumentation and Control Division, NASA Glenn Research Center, organization code 5530, 216–433–3740.

12a. DISTRIBUTION/AVAILABILITY STATEMENT

Unclassified - Unlimited
Subject Category: 07 Distribution: Nonstandard

Available electronically at http://gltrs.grc.nasa.gov

This publication is available from the NASA Center for AeroSpace Information, 301–621–0390.

12b. DISTRIBUTION CODE

13. ABSTRACT ***(Maximum 200 words)***

In this report, a fault detection and isolation (FDI) system which utilizes a bank of Kalman filters is developed for aircraft engine sensor and actuator FDI in conjunction with the detection of component faults. This FDI approach uses multiple Kalman filters, each of which is designed based on a specific hypothesis for detecting a specific sensor or actuator fault. In the event that a fault does occur, all filters except the one using the correct hypothesis will produce large estimation errors, from which a specific fault is isolated. In the meantime, a set of parameters that indicate engine component performance is estimated for the detection of abrupt degradation. The performance of the FDI system is evaluated against a nonlinear engine simulation for various engine faults at cruise operating conditions. In order to mimic the real engine environment, the nonlinear simulation is executed not only at the nominal, or healthy, condition but also at aged conditions. When the FDI system designed at the healthy condition is applied to an aged engine, the effectiveness of the FDI system is impacted by the mismatch in the engine health condition. Depending on its severity, this mismatch can cause the FDI system to generate incorrect diagnostic results, such as false alarms and missed detections. To partially recover the nominal performance, two approaches, which incorporate information regarding the engine's aging condition in the FDI system, will be discussed and evaluated. The results indicate that the proposed FDI system is promising for reliable diagnostics of aircraft engines.

14. SUBJECT TERMS

Aircraft engines; Fault detection and isolation; Health monitoring

15. NUMBER OF PAGES

41

16. PRICE CODE

17. SECURITY CLASSIFICATION OF REPORT	18. SECURITY CLASSIFICATION OF THIS PAGE	19. SECURITY CLASSIFICATION OF ABSTRACT	20. LIMITATION OF ABSTRACT
Unclassified	Unclassified	Unclassified	